POLITECNICO DI TORINO

Master's Degree in in Mining Engineering

Politecnico di Torino

Master's Degree Thesis

A numerical method for potential implementation of underbalanced drilling in high pore pressure reservoirs

Supervisor:
Prof. Marilena Cardu

Prof Chiara Deangeli

Candidate:
Oveis Farzay

July 2022

Acknowledgements

This project would not have been possible without the support of many people. I would like to express my gratitude and appreciation to all those who gave me the possibility to complete this report. Special thanks are due to my supervisors **Prof. Marilena Cardu** and **Prof. Chiara Deangeli** whose support, stimulating suggestions, and encouragement helped me during the process of writing this report.

Many thanks go to the whole lecturers and professors at DIATI Department of the Politecnico di Torino who opened my mind to new aspects of my study and guided me towards achieving my goals. I would like to specially thanks to **Seyedalireza Khatibi** from Petroleum Engineering Department, University of North Dakota and **Adel M. Al-Ajmi** Department of Petroleum & Chemical Engineering, Sultan Qaboos University whom I had the privilege of working with in this thesis. My profound thanks go to all classmates, especially to my friends for spending their time in helping and giving support whenever I need it in fabricating my project.

Last but not least, my family deserves endless gratitude: my father for encouraging me to be what I want to be, my mother for supporting me no matter what. To my family, I give everything, including this.

Table of Contents

List of figures

List of tables

Abstract

The growing number of depleted reservoirs around the world and the increasing necessity to recover hydrocarbons more efficiently has been forcing the oil and gas industry to continuously improve its drilling technology.

Due to vast application of overbalanced drilling (OBD) and the facilities that are more accessible logistically, the benefits that Underbalanced drilling (UBD) can bring for the reservoir production are often ignored. Especially when it comes to high pressure reservoir, more often drillers are prone to use OBD than UBD due to less cost and challenges.

A reliable MEM as an indicator of Wellbore ability to withstand mechanical problems in either high pressure or normal pressure reservoir, can be used to investigate UBD feasibility study. Once the feasibility of UBD approved, an alternative option for drilling such reservoir can be highlighted.

UBD is a drilling process in which the mud weight of drilling fluid is intentionally less than the formation fluid density of the being drilled. This underbalanced pressure condition allows the reservoir fluids to enter the wellbore during drilling, thus preventing fluid loss and related causes of formation damage.

In this study, a numerical simulation using Finite-difference model (FLAC 3D code) is applied to evaluate the feasibility of UBD in high pore pressure reservoirs in real field. To achieve this objective, the minimum possible mud weight that ensures wellbore stability is estimated by considering an elastoplastic model. The growth of the plastic area around the wellbore is studied and utilized as an indicator of wellbore instability. Moreover, a detailed study is conducted in the zones with no safe mud windows to determine the optimum mud weight.

Keywords: Underbalanced drilling, Numerical simulation, High pore pressure reservoir, Elastoplastic model, Plastic zone.

1. Concept and general aspects

1.1. Introduction

Wellbore instability while drilling is one of the costliest phenomena that is facing the petroleum industry. Due to the increasing maintenance costs required to stabilize the wells' wall, petroleum companies have shown a greater tendency to use open wells (without supports), so it is necessary to know all the parameters affecting the stability of wells.

Wellbore instability depends on the distribution and concentration of stress around the drilled well. If the rock strength is greater than the induced stresses, the well will remain stable, otherwise it will fail. Factors influencing wellbore instability can be listed in two general categories: Controllable factors and Uncontrollable.

Controlling the stability of the wellbore wall requires an understanding of the interaction between rock strength and in-situ stresses. Since in situ stresses and rock strength cannot be controlled, the only way to prevent wall rupture during drilling is to obtain optimal well trajectory and the optimal mud weight range.

In underbalanced drilling, the drilling fluid pressure is designed to be lower than formation pore pressure, which raises the chance of borehole instability. Accordingly, the analysis of wellbore stability is essential before carrying out an underbalanced drilling operation.

1.2. Importance of wellbore stability analyses

Drilling for the purpose of oil and gas extraction under complex geological conditions reveals the importance of wellbore stability. The consequence of such a phenomenon can be economical due to the creating Non-Productive Time (NPT) or even loss of well and shutting down the project. New technologies that are implemented in oil and gas industry, like under balanced drilling, high pressure drilling jets, horizontal wells, and multi-lateral wells are raising the demand for wellbore stability studies. The wellbore stability study should be done prior to drilling, while drilling, and after completion towards the well life (Figure 1).

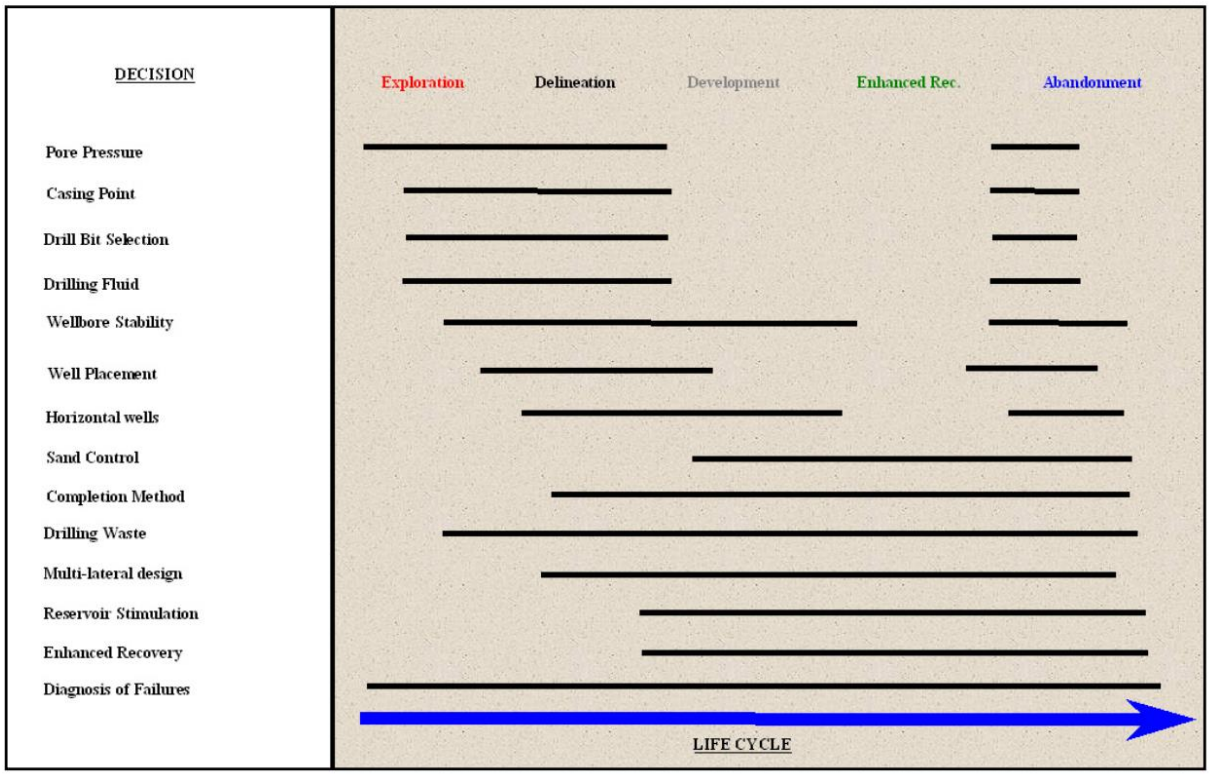

Figure 1 Geomechanics scope for the life of a field (Ajah, Dosunmu et al. 2020).

Some important benefits of wellbore stability analysis are:

- Reducing costly drilling problems such as drilling bit stuck, bit losses, undesired excessive well diameter and hydraulic problems.
- Reducing the exploration risk and analyzing the subsidence.
- Optimizing the mud weight, reducing the probability of damages to the main formation
- Enhance reservoir production, induced the probability of production from faults.
- Minimizing the collapse and fracture in wellbore wall and consequently lessen the probability of stuck.
- Avoiding both depletion and loss pressure head.

Vice versa, the consequence of ignoring such analyses can be catastrophic, as listed in Table 1.

Table 1 Consequence of ignorance of wellbore stability analyses(Papanastasiou and Zervos 2005).

Uncontrollable (Natural) Factors	Controllable Factors
Naturally Fractured or Faulted Formations	Bottom Hole Pressure (Mud Density)
Tectonically Stressed Formations	Well Inclination and Azimuth
High In-situ Stresses	Transient Pore Pressures
Mobile Formations	Physico/chemical Rock-Fluid Interaction
Unconsolidated Formations	Drill String Vibrations
Naturally Over-Pressured Shale Collapse	Erosion
Induced Over-Pressured Shale Collapse	Temperature

The mission of the Wellbore Stability is to Minimize the "learning curve" when developing new reservoirs so that optimal well costs are obtained early on.

- Identify potential drilling problems during the well planning stage
- planning can be developed to minimize costs associated with wellbore stability problems.

The causes of wellbore instability are often classified into mechanical (failure of the rock around the hole because of high stresses, low rock strength, or inappropriate drilling practice) or chemical, which arise from damaging interaction between the rock, generally shale, and the drilling fluid. Often, field instances of instability are the result of a combination of both chemical and mechanical. This problem might cause serious complication in well and in some case can lead to expensive operational problems (Pašić, Gaurina Međimurec et al. 2007).

Chemical instability is the control of the drilling fluid/rock interaction, and it's usually most problematic when drilling shales are encountered. Shales are fine grain sedimentary rocks with very low permeability and composed primarily of clay minerals (gumbo to schistose siltstone).

One factor that distinguishes shale from other rock is its sensitivity to the water component of drilling fluids. With time, shale/water interaction will decrease the strength of the shale, making it more prone to mechanical stability failure. As shale is drilled, a sequence of events take place that can lead to the stressing, weakening, and eventual failure of the shale.

Mechanical stability problems directly account for many unscheduled rig events. Stability problems also effect overall drilling efficiency by altering the shape of the hole being drilled. Severe hole deformation occurs when extreme stress environments are penetrated. Figure 2 is

indicative of such drilling. Consider the path of a typical well and consider this deformation over several thousand feet of open hole; it is easy to see the impact of such a wellbore on operations.

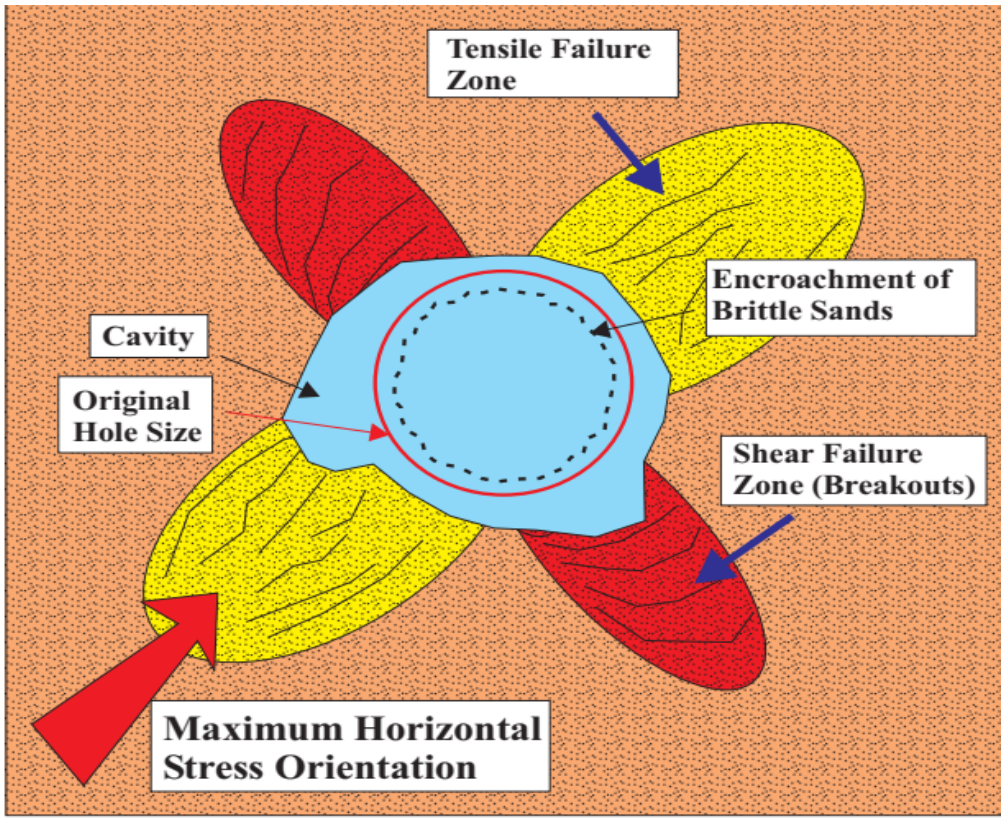

Figure 2 Mechanical instability possible to occur in wellbore (Pašić, Gaurina Međimurec et al. 2007).

1.3. Indicators of wellbore instability

A list of the indicators of wellbore instability which are primarily caused by the wellbore instability or convergence during the drilling, completion or production of a well is shown in Table 2. The indicators of instability are classified in two groups: direct and indirect causes. Direct symptoms of instability include observations of over gauge or under gauge hole, as readily observed thanks to caliper logs. Caving from the wellbore wall, circulated to surface, and hole fill after tripping confirm that spalling processes are occurring in the wellbore. Large volumes of cuttings and/ or carvings, in excess of the volume of rock which would have been excavated in a gauge hole, similarly attest the hole enlargement. Provided that the fracture gradient was not exceeded and that no naturally fractured formations were encountered, a requirement for a cement volume in excess

of the calculated drilled hole volume is also a direct indication that enlargement has occurred (Pašić, Gaurina-Međimurec et al. 2007).

Table 2 Indicators of wellbore instability (Pašić, Gaurina-Međimurec et al. 2007).

Indicators of wellbore instability	
Direct indicators	**Indirect indicators**
Oversize hole	High torque and drag (friction)
Under gauge hole	Hanging up of drill string, casing, or coiled tubing
Excessive volume of cuttings	Increased circulating pressures
Excessive volume of carvings	Stuck pipe
Caving's at surface	Excessive drill string vibrations
Hole fill after tripping	Drill string failure
Excess cement volume required	Deviation control problems
Inability to run logs	
Poor logging response	
Annular gas leakage due to poor cement job	
Keyhole seating	
Excessive doglegs	

1.4. Technical terms

Formation Pressure (P_f): The pressure of fluids within the pores of a reservoir is called reservoir pressure or pore pressure. Formation pressure tends to increase according to the hydrostatic pressure gradient, in this case 0.433 psi/ft. Deviations from the normal pressure gradient and its associated pressure at a given depth are considered abnormal pressures.

Normal Formation Pressure: the pressure of a column of water extending from the formation to the surface is called normal pressure. Normal formation pressure gradient is 0.433 psi/ft. for fresh water and 0.465 psi/ft. for seawater.

Abnormal Pressure: A pressure gradient less than 0.433 psi/ft is called subnormal pressure. Abnormal pressure is the condition in which the pore pressure of a geologic formation exceeds or is less than the expected, or normal, formation pressure.

Hydrostatic Pressure (P_h): It's the pressure due to the weight of mud column under static condition.

Bottomhole Pressure (BHP): BHP is the pressure at the bottom of the well and usually it's measured in pounds per square inch (psi). This pressure may be calculated in a static, fluid-filled wellbore with the equation:

$$Equation\ 1 \quad P_{bh} = 0.052\rho \times h$$

Figure 3 shows the terms explained above.

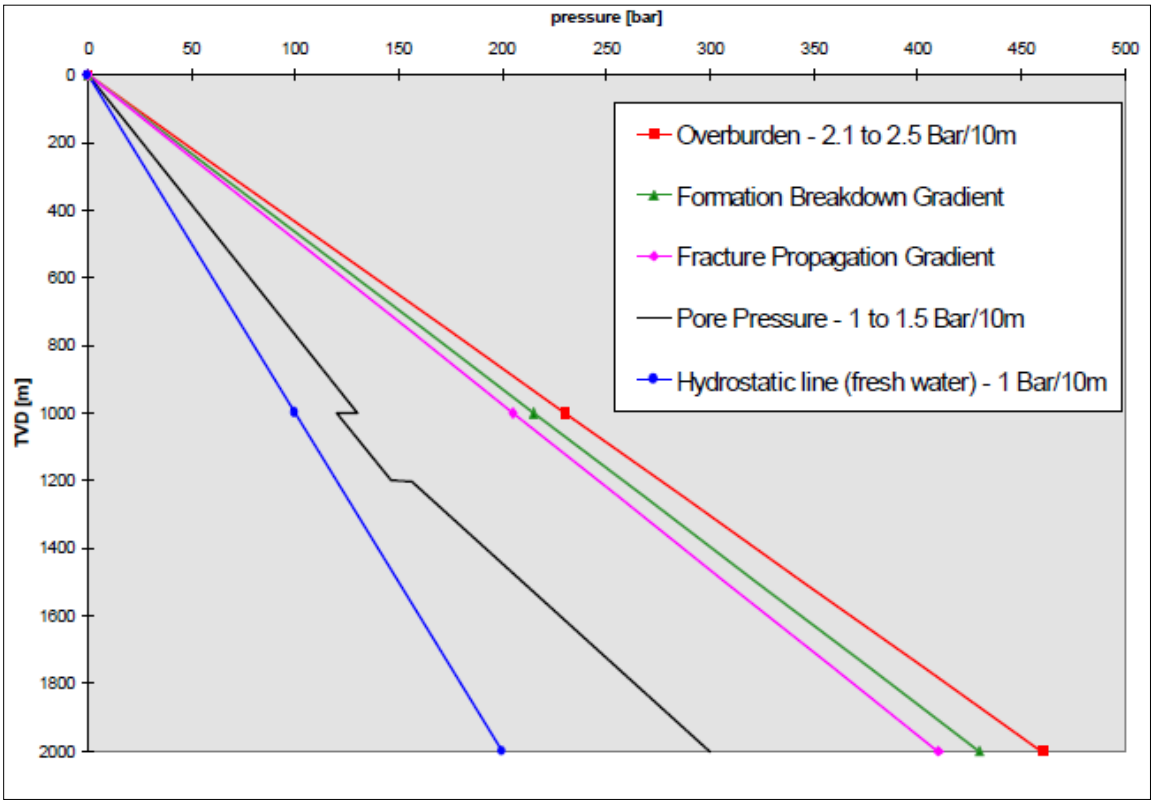

Figure 3 Illustration of pressure versus depth (Blanton and Olson 1999).

1.5. Drilling methods

There are different approaches to drill a well. In general, they can be divided into three categories: conventional, managed pressure, and underbalanced drilling. Figure 4 shows a simplified pore pressure plot. The x-axis represents the pressure, while the y-axis represents the depth. The three lines shown in the plot represent different pressure boundaries. The brown "Borehole Stability" line corresponds to the formation collapse pressure, the blue "Pore Pressure" line corresponds to the formation pressure and the red "Frac or Lost Circulation" line corresponds to the formation fracture pressure. The different colors represent the drilling windows for three different drilling techniques.

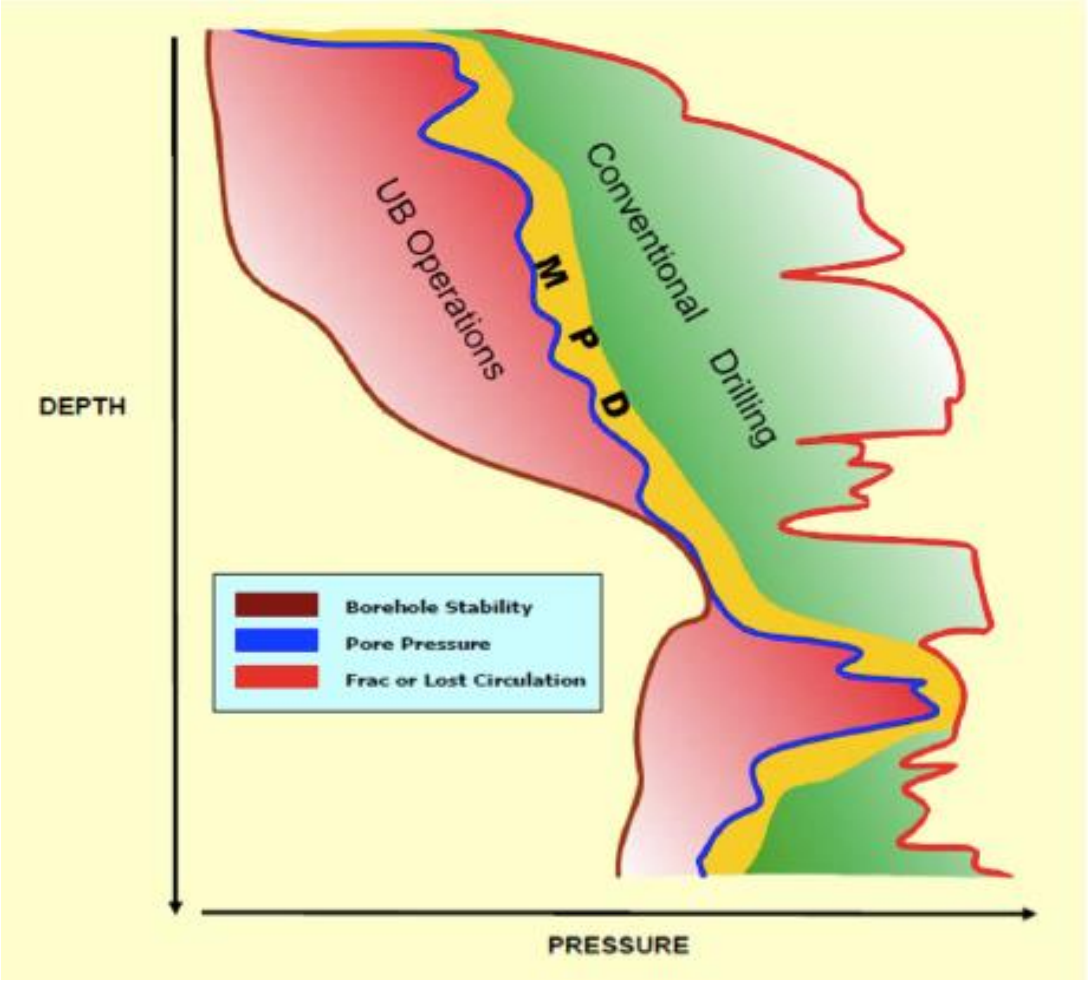

Figure 4 Pore Plot Illustrating Different Drilling Methods (Malloy, Stone et al. 2009).

1.5.1. Conventional Overbalanced Drilling (OBD)

Conventional overbalanced drilling is the most common drilling practice used in the drilling industry. In Figure 4, the conventional drilling window is shown with the green color, between the pore pressure line and the fracture pressure line. This is also how conventional overbalanced drilling is defined. The pressure exerted in the wellbore is greater than the formation pressure in any part of the wellbore. By keeping a hydrostatic pressure above the formation pressure, the formation fluid will be kept in the formation by the positive differential pressure. Adjusting the mud weight and mud pump pressure during drilling operations controls the overbalanced pressure. There are, however, other concerns. As Figure 4 shows, there is an upper pressure boundary, i.e., the formation fracture pressure. If the mud weight exceeds the formation fracture pressure during drilling, the formation may fracture giving a new flow path for the mud with the result of loss of circulation. Therefore, to the mud loss, the well may become unintentionally underbalanced, and the well may take a kick. Drilling well sections with a narrow drilling window between pore and fracture pressure are therefore a major challenge using conventional drilling methods. As mud weight is static until casing setting depth is reached; one problem is to run out of casing sizes before target depth is reached.

1.5.2. Managed Pressure Drilling (MPD)

The MPD drilling window is shown in Figure 4 by the yellow color. As for conventional overbalanced drilling, it aims to keep the wellbore pressure above the formation pressure and at the same time below the formation fracture pressure. However, the MPD approach does not require the big drilling window, as for the case with conventional drilling. Narrow drilling windows are often found in deep water drilling and in depleted formations: conventional drilling here could cause a great risk of resulting in an unintentional kick induced by either to low mud weight or due to mud losses from fracturing the formation. The MPD technique gives, as the name states, the opportunity of managing the bottom-hole pressure from surface while drilling.

1.5.3. Underbalanced Drilling (UBD)

The definition of underbalanced drilling stated by the IADC Underbalanced Operations committee is: “Drilling with the hydrostatic head of the drilling fluid intentionally designed to be lower than the pressure of the formations being drilled”. The hydrostatic head of the fluid may naturally be

less than the formation pressure, or it can be induced. The induced state may be created by adding natural gas, nitrogen, or air to the liquid phase of the drilling fluid. Whether the underbalanced status is induced or natural, the result may be an influx of formation fluids which must be circulated from the well and controlled at the surface. In terms of pressure, underbalanced drilling can be described with the following equation:

Equation 2 $P_{formation} > P_{BHP} = P_{mud} + P_{friction} + P_{choke}$ *(Aadnoy and Engineers 2009)*

The main differences between UBD and conventional overbalanced drilling (OBD) are that the drilling mud doesn't act as a barrier against the formation pressure, and this allow influx of formation fluids into the well. In addition, there are many other differences that develop due to these two main differences. Figure 4 shows the operating area for underbalanced drilling, which is below the pore pressure and above the collapse pressure.

1.6. Evolution of underbalanced drilling

A few wells drilled initially in eighteenth century were drilled underbalanced. These wells were operated with fluid column pressure in the annulus compared to the adjacent formation, but they collapsed as the well flowed through a permeable zone: being an uncontrolled flow, this resulted in lost reserves. The earliest underbalanced operation patent can be traced back to the mid-1800s.The patent was issued for using compressed air to clean out cuttings from the bottom of a hole. Advances in the UBD continued in the exploration of hydrocarbon throughout the mid-1900s. Then, using mist and multiphase fluids to control downhole fires in air/gas fluid operations started and provided a higher tolerance to water influxes. Algorithms and equations were developed to predict the amount of gas required to clean the holes and the bottom-hole pressure resulting from circulating mixtures of fluid and gas. Progress has been made in understanding and modeling air and multiphase systems. This technological improvement continued in the early 19th century with the first application of multiphase fluids in the 1930s.

Multiphase fluids, air and natural gases mixed with water or oil, became used in oil well operations in the 1930s. Most fluid system in underbalanced operations was first introduced in late 1930s. Drilling underbalanced with pure air or natural gas also increased at this time. Closed systems were started to capture the fluids produced and improve safety. Foam entered an underbalanced operation fluid system in the 1960s due to its characteristics of better hole-cleaning ability than air and multiphase systems. UBD technology was used in limited applications before 1970s.

Limitations were due to environmental problems, particularly in gas fluid systems, where large amounts of dust were released into the atmosphere. In single-circulation foam systems, the waste generated was a serious concern. Most unbalanced wells drilled before 1985 were characterized by low pressure applications. The main objective of many of these applications was to increase the penetration rate (ROP) in non-productive areas

New technologies developed in the late 1980s and 1990s were characterized by a re-emergence of UBD, with improvements in multiphase modeling capabilities and the development of high-pressure rotating control heads. Rotating heads have been available in the drilling operation industry for decades, but innovation since 1987 has led to the development of rotating control devices capable of withstanding up to 3,000 psi when drilling. Thus, this pressure rating of the RCD has greatly expanded the applicability of underbalanced operations

Since then, underbalanced operations have proven to be an effective technology in minimizing damage during horizontal well operations. The technology has been attempted throughout South America, the Middle East, and Southeast Asia. Several UBD projects have also been completed in Africa, Australia, and Europe. Underbalanced operations were introduced into the offshore environment by Shell in the late 1990s.

1.7. Benefits and limitation of UBD

1.7.1. Advantages

Underbalanced Drilling Technology offers the following benefits:

- **Enhancement to the ultimate recovery**

Final recovery improvement is the dream of all Reservoir Engineers. This effect, admittedly, is not easy to quantify. However, Underbalanced Drilling Technology improves the final recovery (Aadnoy, Cooper et al. 2009).

- **Discovery of new zones**

There are many cases where zones are drilled conventionally, and look “good” on a log, but they produce little or nothing. Most well site geologists can cite cases like this. Even if the zone is tested, it may not flow if it is sufficiently damaged with overbalanced fluid. Under such circumstances, the reserves of the zone must be considered as zero. Drilling through the same

underbalanced zone may show that it is productive at commercial rates. The hydrocarbon in that zone therefore may be counted as new reserves, based on using the Underbalanced Drilling Technology.

- **Reducing Formation Damage and increasing intra-zone contribution**

Because unbalanced drilling minimizes drilling-induced formation damage, it allows the reservoir to produce virtually intact. Therefore, it eliminates the need to stimulate wells to obtain economical production. It should be emphasized that unbalanced drilling is optimally applied in combination with horizontal drilling techniques.

As regards the increase in intra-zone contribution, this is the reduction of the zone contribution due to skin damage. This reduction is more pronounced in tight and/or layered reservoirs. If, for example, a skin-damaged zone within a layered production reservoir has prevented hydrocarbons production, the well reserves are reduced by the amount that zone does not contribute. Underbalanced technology, on the other hand, reduces or eliminates the damage, allowing the hydrocarbon of that zone to be added as reserves.

- **Lower abandonment pressure**

Reserves may be added, especially in gas fields, by reducing abandonment pressure. The contribution of underbalanced drilling technology to abandonment pressure reduction comes from either:

- ❖ Reducing skin and/or increasing production of infill wells (relative to a conventionally drilled well).
- ❖ Allowing wells to be drilled late in reservoir life (for the purpose of abandonment pressure reduction), that could not successfully be drilled any other way.

- **Increase well Drainage area**

When the wells are in interference, underbalanced drilling increases the drainage area of a single well versus competing conventional wells. Therefore, reservoir engineers would be able to optimize the number of wells and their spacing.

- **Access to challenging reservoirs**

Some reservoirs are difficult to access using conventional drilling techniques. Therefore, access is the only major reserve contribution related to underbalanced drilling with respect to reservoirs that could not be drilled conventionally. In almost all cases, underbalanced is highly recommended in the following situation, only after the conventional well has proved expensive and unsuccessful:

- ❖ Low pressure / severely depleted reservoirs.
- ❖ Highly fractured reservoirs.
- ❖ Reservoirs with a narrow margin between fracture pressure and pore pressure.

The "test" for whether reserves are added through "access" is very simple: if a conventionally drilled well can be drilled at a reasonable cost and recover the reserves, underbalanced is assumed not to have a value in reserve additions. If, on the other hand, conventional wells are uneconomic due to lost circulation, fishing, and other problems, and the project is uneconomic with conventional wells, but is economic when drilled underbalanced, there is a reserve contribution from underbalanced drilling technology.

It should be emphasized that intra zone contribution, abandonment pressure relief, and access are all somewhat related in some way, and are not necessarily separate and distinct effects, but these categories may be useful for evaluating reserves.

- **Real time reservoir evaluation / characterization**

Most reservoir characterization techniques try to infer bulk reservoir properties instead of measuring them directly:

- ❖ Logs measure electrical/acoustical/nuclear properties, not porosity or pore fluid composition.
- ❖ The core analysis determines the properties of a very limited section of the reservoir under conditions very different from those experienced in-situ.

On the other hand, underbalanced drilling allows the reservoir to be characterized by measuring the productivity, which is one of its most important features.

Underbalanced drilling offers an unprecedented opportunity to examine a reservoir as it is being drilled. With proper data acquisition and engineering interpretation, underbalanced drilling allows personnel to locate and identify geological anomalies such as fractures, tight zones, pinch outs, discontinuities, and water zones (Saponja 1998). Reservoir and production engineers can use this information to determine:

- ❖ Degree of reservoir heterogeneity.
- ❖ Productivity Index while Drilling.
- ❖ Optimum horizontal well bore length (based on productivity)
- ❖ Number & orientation of future development wells.
- ❖ Anticipated production rates.

- **Increased rate of penetration**

Rate of penetration (ROP) increases with UBD. The pressure in the formation and the resulting flow will make it easier to drill "loose" the cuttings so that the drilling will occur faster. Since drilling often will be done with solids-free mud, reduced bit wear is expected. In some hard rock formations, a significantly higher ROP can be achieved with UBD (Figure 5). This reduces the time needed for drilling the well, and therefore the total cost of the well (Aadnoy and Engineers 2009).

Figure 5 ROP for UBD and OBD (Aadnoy, Cooper et al. 2009).

- **Narrow pressure window**

In some formations, the difference between the pore pressure and the fracture pressure is very small. This can be natural or it can be caused by, for example, a fluid injection (Eck-Olsen, Vollen et al. 2004) . This is called a narrow drilling window, as shown in the lower part of Figure 5. In such situations, conventional overbalanced drilling can be very difficult to perform. Small variations in BHP can cause either fracturing of the formation and mud losses, with possibility for well control issues, or can get a kick due to too low pressure. Underbalanced drilling can avoid these problems. One can get any mud losses since always have a BHP lower than the fracture pressure limit. Using appropriate equipment to handle the continuous influx from the reservoir, will not be a problem either.

- **Avoiding differential sticking**

The filter cake is formed on the wellbore, as filtrate leaks out of the drilling mud into the formation. This is a typical operational phenomenon for overbalanced drilling. Filtrate is a clear or colored liquid with very little solid content. When the liquid filtrate leaves the drilling mud, the clay and barite solids in the mud that are left behind on the wellbore form a relatively impermeable cake, called filter cake. Filter cake continually builds up and then is abraded by the rotation or sliding of drill pipe and by the flow of drilling mud. Differential sticking occurs when the drill stem comes to rest against filter cake in an overbalanced hole. Low pressure on the reservoir side pulls, while high pressure on the wellbore side pushes the pipe to the side of the hole. When the pressure in the well is higher than the formation and there is a mud cake to transmit the pressure differential to the formation, the possibility of getting stuck occurs, especially in the diverted holes where the drill string is resting on the lower side of the wellbore. In Under balanced drilling neither an overbalance nor a mud cake exists, hence avoiding this problem is predictable (Aadnoy and Engineers 2009).

1.7.2. Disadvantages with UBD

There can be some disadvantages tied to underbalanced drilling. These problems are often due to the result of a poorly planned and executed UBD process, and can many times be mitigated by good planning and designing.

- **Borehole stability problems**

One of the most common problems in UBD is borehole stability problems due to the low pressure in the well. If there is a narrow window between the pore pressure and the collapse pressure and underbalanced operation is adopted, it is easy to get below the collapse border and hole will collapse. This can particularly be a problem when drilling in a depleted reservoir, and the driller encounters a very low pressure in well to stay underbalanced. Borehole instability problems can also be caused by fluctuations in the BHP, gas influx from the formation, drill-string movement, connections, and high annular velocity of the circulating fluid.

High annular velocities can cause washout of the borehole wall. The way to mitigate borehole problems is normally to the case of shale zones that are likely to cause problems and trying to keep the BHP as stable as possible. There are prediction models available for analyzing borehole stability problems and these should be used in the planning of the well (Saponja 1998).

- **Safety issues due to high pressure reservoirs**

When drilling underbalanced, attempt is not to conceal the pore pressure in the formation by creating an overbalance in the hole, instead letting the well flow to the surface. The safety issue then changes from a pressure issue to a flow issue. In reservoirs with very high pressure and permeability there can be safety issues due to large influx of formation fluids. The equipment on the surface must be able to handle the expected amount of fluid. The safety problem occurs when hitting high pressure or high permeability zones which is not expected. So, problems can arise with handling surface fluids that have not been planned, and where equipment has insufficient contingency.

- **Development of tensile stress near a wellbore**

Unexpected overpressures can induce tensile stresses around the wellbore, and the selection of an appropriate strength criterion and rock properties play an important role in determining the limit mud pressures(Deangeli and Marchelli) .

- **Use of MWD**

In UBD, gas or gasified mud will often be used as the drilling fluid. Conventional MWD depends on a non-compressible fluid as a signal transmitter and therefore will not function properly in a compressible fluid such as gas. This problem can be avoided using EM MWD – electromagnetic MWD, or wired drill pipe (Graham, 2011).

- **Failure to maintain a continuous under-balance in the well**

If driller cannot keep a continuous under-balance in the well it can lead to severe formation damage due to invasion of drilling fluid into the formation. Since the mud cake does not exist, while drilling underbalanced the formation damage most likely will be much worse than the damage caused by a normal overbalanced drilling operation. The reason for getting into overbalance can be due to things like making connections, bit trips or local undetected depletion zones (Bennion, 1999).

- **Cost of UBD operation**

A UBD operation is significantly more expensive than a conventional OBD operation. The reasons for that are due to the extra equipment needed and to the more comprehensive planning process. This is perhaps the most common reason for not drilling underbalanced. The cost of the UBD operation must be weighed against the benefits it can provide before making a decision. If it is possible to obtain a good result with conventional drilling, this method should be chosen. Another alternative is to use managed pressure drilling (MPD) which in many cases can be less expensive and provide very good results.

1.8. Previous studies

Wellbore instability is one of the most problematic issues in petroleum industry during drilling and production operations. In the literature, the wellbore instability is generally considered to be a mechanical problem, physico-chemical problem or both (Zeynali 2012). In these cases, the factors affecting the wellbore instability are classified as controllable and uncontrollable. With respect to the mechanical wellbore stability, the in situ stresses, the pressure of the formation pores and the mechanical properties of the rock are uncontrollable factors, while the well pressure and the trajectory of the well are taken as controllable parameters in the stability analysis (Khatibi, Aghajanpour et al. 2018). The most important study regarding the wellbore stability analysis is listed in Table 3.

Most of wellbore stability analysis studies focused on the controllable parameters to avoid the borehole collapse during drilling and to prevent sanding during the production stage (Alexeyev, Ostadhassan et al. 2017, Khatibi, Ostadhassan et al. 2019). In addition to this, the study of the optimum well trajectory with minimum fracture gradient during the production phase is essential. Therefore, a path that has the minimum mud pressure to avoid the borehole collapse (i.e., collapse pressure) during drilling and, at the same time, which provides the minimum fracture gradient during the production represents the overall optimum well trajectory.

Furthermore, many studies have been conducted on wellbore stability analysis for special drilling operations and conditions (Hareland and Dehkordi 2007, Khatibi, Farzay et al. 2018), for instance, combining an elastoplastic model with a finite-explicit code (FLAC) and estimating an optimum equivalent circulating density (ECD) to avoid instability during underbalanced drilling (UBD). He, Wang et al. (2015) covered the impact of fluid seepage on wellbore stability during underbalanced drilling and proposed a new model for collapse pressure determination in UBD of horizontal wells. In underbalanced drilling, the fluid pressure is designed to be lower than formation pore pressure, which raises the chance of borehole instability. Accordingly, the analysis of wellbore stability is essential before carrying out an underbalanced drilling operation. To assess the wellbore stability, linear elastic model (LEM) is often applied due to its simplicity and the requirement for few input parameters (Soliman and Boonen 2000).

In some applications, elastoplastic models are adopted and reported to improve the evaluation of wellbore instability (Al-Shaaibi, Al-Ajmi et al. 2013). Elastoplastic models are distinguished by counting the post-failure behavior of rocks and their ability to withstand higher stress concentration (Westergaard 1940, Risnes, Bratli et al. 1981, Hsiao 1988, Bradford and Cook 1994, Bradford and Cook 1994, Hawkes and McLellan 1996, McLellan, Hawkes et al. 2000, Crook, Yu et al. 2002, Aghajanpour, Fallahzadeh et al. 2017, Khatibi, Aghajanpour et al. 2018).

As there were successful cases in which high-pressure reservoirs were drilled UBD (Urselmann, Cummins et al. 1999), a numerical method for potential implementation of underbalanced drilling in high pore pressure reservoirs is studied in this work. A finite explicit simulator, that is FLAC 3D, is employed to conduct the wellbore stability simulation. In the numerical modelling, an elastoplastic model coupled with the Mohr-Coulomb failure criterion is adopted.

A normalized yielded zone area (NYZA), defined as the ratio of cross-sectional area of the plastic zone to the original area of the wellbore, is used as an indicator for the growing of the plastic zone.

In this regard, well deviation, operation settings and hole cleaning capacity have a great impact in the development of the plastic zone (Hawkes and McLellan 1996, Hawkes and McLellan 1999, Hawkes, Smith et al. 2002). Furthermore, experiments showed that as the plastic zone and consequently NYZA become larger, wellbore stability decreases (Hawkes, Smith et al. 2002, Chen and Abousleiman 2016).

In addition, there is a NYZA corresponding to a low mud weight that is required to stabilize the well (McLellan and Hawkes 1999, Alquwizani and Sharma 2014). If the mud weight is less than the pore pressure, UBD will be feasible regardless of other operational restrictions. In this work, a real field case study is conducted in a high-pressure reservoir utilizing the FLAC simulator to examine UBD potential in the field.

Table 3 Current wellbore stability models.

Reference	Model type	Special features
(Bradley 1979)	Linear elasticity	Zero tensile strength
(Fuh, Whitfill et al. 1988)	No chemical effect	
(Aadnoy and Chenevert 1987)	No fluid diffusion	Zero tensile strength
(McLean and Addis 1990)	No thermal effect	
(Zhou, Hillis et al. 1996)		Truncated Desai's yield function
(Santarelli, Brown et al. 1986)	Stress dependent linear elasticity	
(Detournay and Cheng 1987)	Linear poroelasticity	Vertical well Undrained condition
(Yew, Chenevert et al. 1990)	Moisture adsorption	
(Wang 1998)	Chemical effect and moisture adsorption	Variable Young's modulus
(Yew and Liu 1992)	Linear poroelasticity, no chemical effect	
(Mody and Hale 1993)	Chemical effect	Stress on the wellbore wall
(Sherwood 1993)	Chemical effect	Chemical potential of different components
(Wang and Papamichos 1994)	Chemical effect	Shale properties vary with water content
(Cui 1997)	No chemical effect	Solution in Laplace domain, superposition technique
(Cui, Abousleiman et al. 1999)	Time dependency	
(McLean and Addis 1990)	Nonlinear elasticity	
(McLellan 1996)	Elasto-Plasticity	
(McLellan and Wang 1994)	Elasto-Plasticity Plasticity	
(Ewy, Ray et al. 1999)	Coupled thermohydro-poroelasticity	Drained and undrained conditions
(Wang, Papamichos et al. 1996)	Thermoporoelasticity	Conductive heat flow
(Choi and Tan 1998)	Thermoporoelasticity	Numerical validation
(Wang and Dusseault 1995)	Thermoporoplastic	

1.9. Assumptions of the study

1. The loss of mechanical equilibrium causes the deformation and failure of wellbore. No fluid flow, thermal effects, chemical effects and man-made effects are considered during the drilling process. The only hydraulic effect of the drilling mud is to provide hydrostatic pressure support to the borehole surface.
2. The material properties are assumed homogeneous and isotropic.
3. Drained condition is assumed, so that the pore pressure change is ignored. Effective stress is used to account for pore pressure.
4. A finite external boundary is large enough to maintain the original in-situ stress on the boundary.
5. Plane strain idealization is used to simplify the problem to 2D, because the stress in the length direction is a constant value. The model considers the stress variation by depth along the block.
6. The wellbore failure is obtained by dilatant shear failure only.
7. The likelihood of wellbore instability is dependent on the area of yielded zone. The greater the yield, the greater the risk of having problems with wellbore instability.
8. The Mohr-Coulomb criterion is used.

1.10. Nomenclature

Table 4 Nomenclature.

Abbreviation	Description
α	Biot poro-elastic coefficient
ν	Poisson's Ratio
ϕ	Friction angle
ρ	Formation bulk density
ϵ_x	Strain in the minimum horizontal stress direction
ϵ_y	Strain in the maximum horizontal stress direction
σ_1	Effective maximum principal stress
σ_3	Effective minimum principal stress
σ_h	Minimum horizontal stress
σ_H	Maximum horizontal stress
σ_V	Vertical stress
σ_1 σ_{veff}	Vertical effective stress
g	Gravitational acceleration
z	True vertical depth
ΔT_c	Compressional slowness, us/ft
ΔTs	Shear slowness, us/ft
E	Young's Modulus
G	Shear Modulus
K	Bulk Modulus
APWD	Annular pressure while drilling
DSI	Dipole Shear Sonic Imager
ECD	Equivalent circulating density
FG	Fracture gradient
FMI	Full-bore Formation Micro Imager
FPWD	Formation pressure while drilling
LCM	Lost circulation material
LOT	Leak-off test
LWD	Logging while drilling
MDT	Formation modular dynamic tester
MEM	Mechanical earth model
MWD	Measurement while drilling
NPT	Non-productive time
Pp	Pore pressure
ROP	Rate of penetration
SG	Specific gravity
TD	Total depth
TSTR	Formation tensile strength
UCS	Uniaxial compressive strength
VSP	Vertical seismic profile

2. Mechanical Earth Model (MEM)

The basic approach to Geomechanical analysis is to use the available data for the interpretation of rock strength, stress, and pressures. The key is to insure an internally consistent approach, aimed to the integration and understanding of all the data. In analyzing geomechanics for a field, there are a series of steps that must be followed in order to fully grasp the quality of data and determine the uncertainty coming from data used. Skipping or ignoring the importance of any one of these steps can lead to inconsistencies or poor assumptions in the results.

The development of a Mechanical Earth Model (MEM) is essential in making the best use of field information. The MEM is a description of strengths, stresses, and pressures as a function of depth, referred to a stratigraphic column. Once a MEM is constructed, it can be used to estimate and predict the best possible methods for safely drilling and completing both in a single wellbore and far field development. A typical workflow of the key MEM steps is shown in Figure 6.

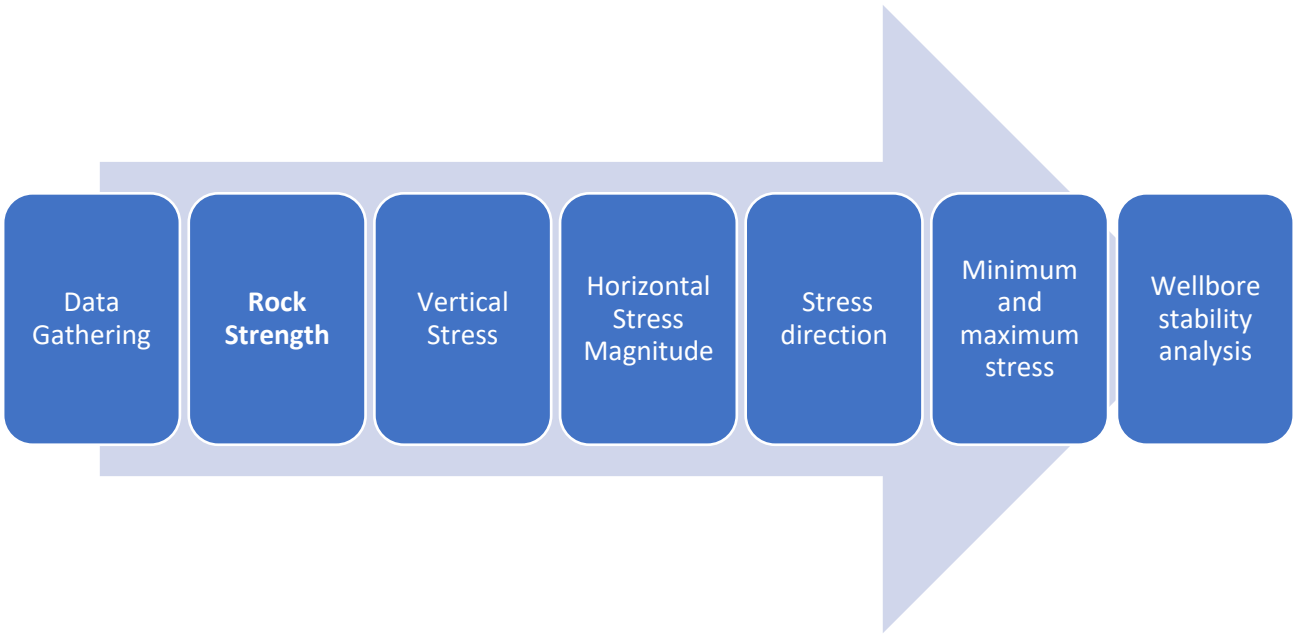

Figure 6 Typical work-flow in the MEM construction process (Castagna and Sun 2006).

In any geomechanical project, a wide range of data may be available for MEM construction and calibration. The typical parameters contained in the MEM and the sources of useful data are listed in Table 5.

Table 5 Input Data for Wellbore stability Analysis.

DATA	No.	Item	Must to Have	Better to Have	Nice to Have
Field	1	Field Layout	Yes		
	2	Full Field Review Report		Yes	
	3	Field Development Plan			Yes
Reservoir	4	Reservoir Pressure		Yes	
	5	Well Test Data		Yes	
Geology	6	Geological Report	Yes		
		Geological			
	7	Cross-Sectional Map			Yes
	8	Image Interpretation Reports			Yes
	9	Well Tops	Yes		
	10	Stratigraphic Column			Yes
	11	Structural Map		Yes	
	12	Geology Related Papers			Yes
Drilling	13	Daily Drilling Report	Yes		
	14	Master Log	Yes		
	15	Mud logging		Yes	
	16	Deviation Survey	Yes		
	17	Stress Measurements (XLOT, LOT, MDT and RFT)		Yes	
	18	Casing and Cementing Diagram	Yes		
	19	Real-Time Drilling Measurements (ECD, ROP, Hook Load, Pump Rate, Pump Pressure and Torque, Mud weight in/out, SPP (stand pipe pressure), ESD, Gas (BG/CG))		Yes	
	20	Cavings, Cuttings or Caving Pictures		Yes	
Processed Well logs and log interpretation	21	Sonic Data (DTSM or synthetic VP/VS relationship and DTCO)	Yes		
	22	Image Data (FMI, FMS, SHDT, UBI and OBMI)		Yes	
	23	Openhole Logs (GR, NPHI, RHOB, CALI, DT,Resistivity or Induction logs)	Yes		
	24	Petrophysical interpretation:Porosities (PHIT, PHIE); Volume fractions (VCL and others)	Yes		
Core	25	Core Data (UCS, Friction Angle, Poisson's Ratio, Young's Modulus, Density, Clay content, Total/effective Porosity)		Yes	
Seismic	26	Cross Line Section		Yes	
	27	Inline Section		Yes	
	28	Interval velocity		Yes	
Production	29	Well Sketch and Completion Design		Yes	
	30	Production and/or injection history (including drawdown and historic reservoir pressure)		Yes	
	31	Workover History		Yes	
	32	Sand Production History		Yes	

2.1. Field case study

The studied field is in the Persian Gulf, 100 km from Iranian shore and 120 km south-west of Bushehr city. Basal forces and salt diapir formed an asymmetrical dome structure with E-W trend. The well is drilled into a shared gas reservoir with geologic age of Late Permian-Early Triassic period, with Dalan and Kangan as the main carbonate reservoir formations. Figure 7 shows the location of the well in a seismic section in time domain, the location of the field in a satellite view of the area, and the stratigraphy column of the reservoir. The well was drilled to provide production from a high-pressure gas reservoir with an initial pressure over 9000 psi.

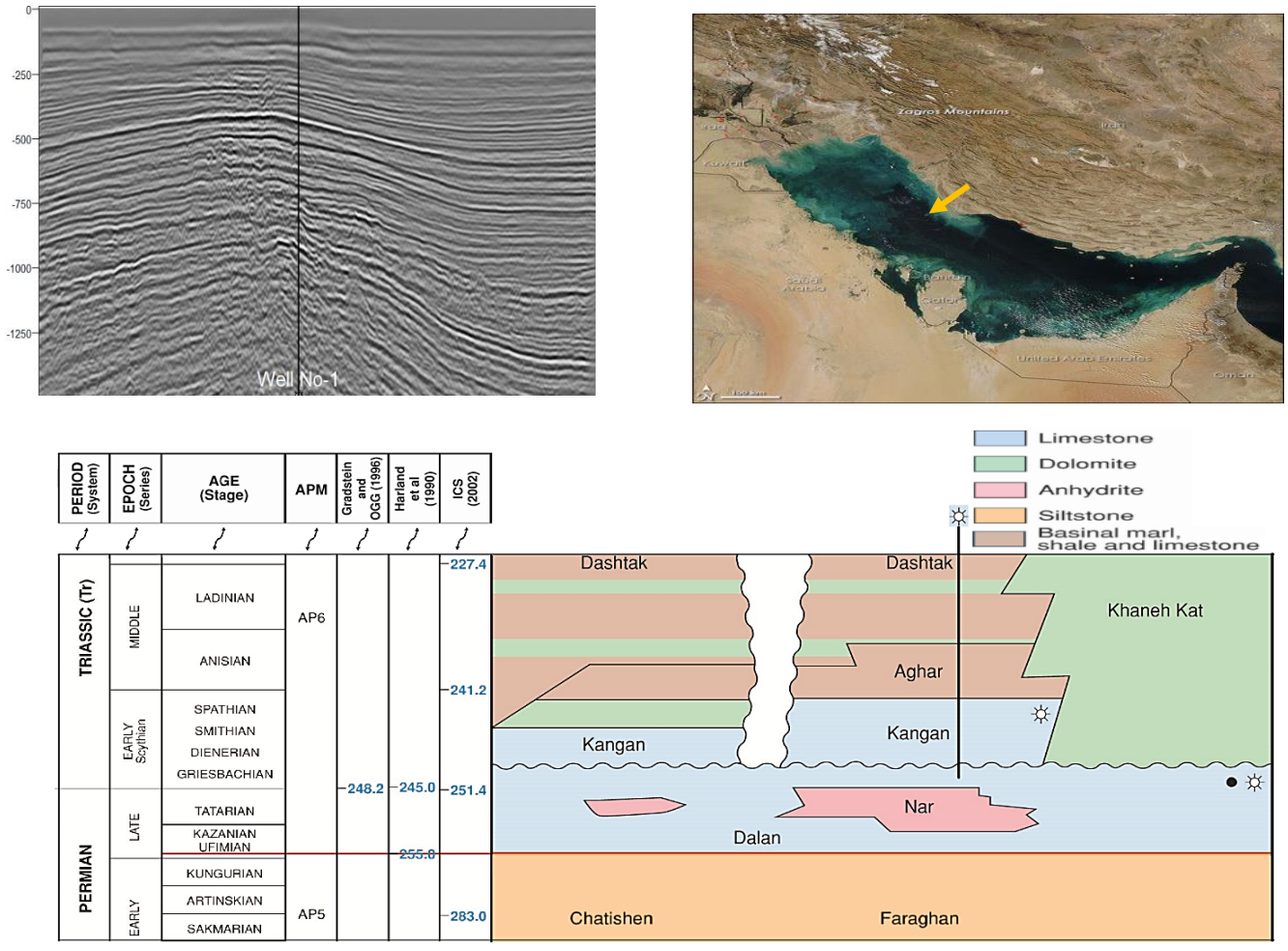

Figure 7 location of the well in the field in time section (ms) (top left); location of the field is shown with an arrow in a satellite view of the area (Top right) and stratigraphy column of reservoir section (bottom).

2.2. Data gathering and quality control

The first step of the study is provided by data collection. Building a Mechanical Earth Model (MEM) requires integrating data from various sources to accurately describe the formations in terms of geomechanical attributes. (Chardac, Murray et al. 2005), provide a guide for appropriate data acquisition when a geomechanical study is required in a field. Data available for the current study include:

1. Formation tops
2. Drilling and completion report
3. Location map and Graphic well logs
4. Final Geological reports
5. Compressional and shear slowness
6. Open hole logs (GR, density, neutron porosity and resistivity...)
7. Static formation pressure data from MDT/XPT tool (reservoir section)
8. Caliper logs
9. Core data

The available log data in well was generally of good quality. Compressional and Shear sonic logs from Sonic Scanner and DSI tools were used for construction of the Mechanical Earth Model.

2.3. 1D MEM

Building a 1 D mechanical earth model (MEM) is the first step for the subsequent procedure to find the optimum mud weight for drilling a well safely. To do so, rock elastic and mechanical properties, pore pressure and in-situ stresses should be estimated as accurately as possible. In this investigation, dynamic elastic moduli such as Young's modulus and Poisson's ratio were calculated using sonic data and bulk density. Then these dynamic properties were converted to static properties based on available correlations along with core measurements from laboratory tests. Rock mechanical properties, such as unconfined compressive strength (UCS), tensile strength and friction angle were also calculated applying the correlation after having provided the core measurements. Reservoir pore pressure was estimated using the pressure gradient obtained from modular formation dynamics test (MDT) for reservoir section and conventional Eaton method for no reservoir sections of the well(Aghajanpour, Fallahzadeh et al. 2017).

Afterward, the vertical stress was calculated based on the weight of overburden layers. In addition, poroelastic horizontal strain model was used to estimate horizontal stresses magnitudes in anisotropic medium. In this study, due to lack of LOT/XLOT and minifrac tests, minimum and maximum horizontal stresses were calibrated with complete mud losses and drilling events in well(Molaghab, Taherynia et al. 2017).

In addition, the maximum horizontal stress direction was detected using full waveform acoustic data and formation micro imager (FMI) log through the wellbore path. Both methods predicted a NW-SE direction for the maximum horizontal stress direction in the reservoir section of the well. After finding the properties by using a proper failure criterion, mud weight boundaries can be determined, in which safe mud weight window would be between breakout and loss limits(Bérard and Prioul 2016). The area of interest for this research was partially held between 2500 m and 4150 m TVD. All the plot that will be shown are in this range of depth. Upcoming parts describes each section in detail.

2.4. Elastic properties

Rock elastic properties represent the basic inputs to the estimation of rock strength and in-situ stresses, which can be later refined and calibrated to other available information. Assuming elastic isotropy, sonic measurements (i.e., compressional slowness and shear slowness) and bulk density were used together with the fallowing equations to calculate the dynamic elastic moduli:

Equation 3 $G = \frac{\boldsymbol{P_b}}{(\boldsymbol{\Delta t_s})^2}$ *Dynamic shear modulus*

Equation 4 $K_{dyn} = \rho_b \left|\frac{1}{(\Delta t_c)^2}\right| - \frac{4}{3} \times G_{dyn}$ *Dynamic bulk modulus*

Equation 5 $\nu_{dyn} = \frac{\frac{1}{2}\left(\Delta t_s / \Delta t_c\right)^2 - 1}{\left(\Delta t_s / \Delta t_c\right)^2 - 1}$ *Dynamic Poisson's Ratio*

Equation 6 $E_{dyn} = 2G(1 + \nu)$ *Dynamic Young's Modulus*

However, these dynamic properties are systematically different from the equivalent static values that are typically needed for subsequent modeling and stress analysis, the dynamic Young's moduli often being 2 to 3 times larger than equivalent static Young's moduli (Plona and Cook 1995, Inc. 1998).

Since rock mechanical tests results for well are available, in the study conversion of dynamic to static Young's moduli (YME) took place using extracted correlation from tests results (Figure 8, Table 6).

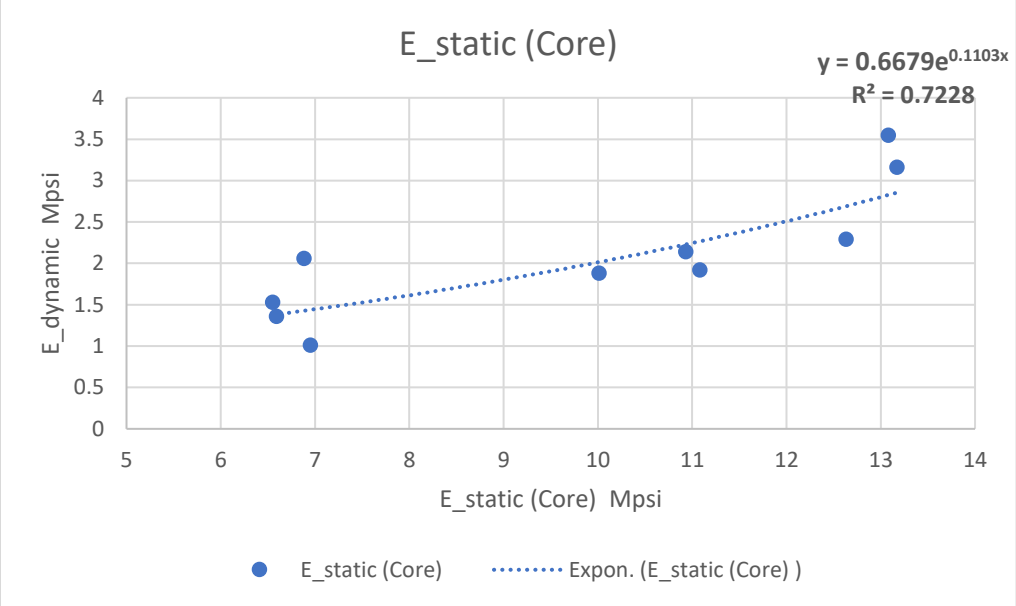

Figure 8 Correlation between dynamic and static Young's Modulus (Mpsi represent 10^6 Psi).

Table 6 Values of dynamic, static (core based) and calculated young's modulus for well (Mpsi represent 10^6 Psi).

E_dynamic Mpsi	E_static (Core) Mpsi	E_s (Calculated) Mpsi
13.17	3.16	2.63
13.08	3.55	2.82
11.08	1.92	2.08
6.59	1.36	1.38
6.55	1.53	1.38
6.95	1.01	1.44
6.88	2.06	1.43
10.01	1.88	1.83
12.63	2.29	2.67
10.93	2.14	2.25

Also, for Poisson's ratio (PR), log derived values calibrated using triaxial compression test's results and static Poisson's ratio (Pr_sta) has been considered as dynamic value multiplied by 0.94 (Table 7).

Table 7 Values of dynamic, static (core based) and calculated Poisson's ratio for well.

Pr_dynamic	Pr_static (Core)	Pr_static (Core)/Pr_dynamic	Pr_static (Calculated)
0.275	0.25	0.91	0.26
0.274	0.27	0.98	0.26
0.245	0.25	1.02	0.23
0.26	0.27	1.04	0.25
0.3	0.25	0.83	0.28
0.27	0.25	0.92	0.25
0.25	0.23	0.92	0.24
Average: 0.267	**Average: 0.25**	**Average: 0.94**	**Average: 0.25**

Biot's constant was assumed to be 1.0 for all formations and rock types considered. This parameter varies from near zero for very stiff zero-porosity rocks (i.e., basalts and pyrite ores), towards a value of near-unity for many porous rocks in shallow sedimentary basins.

Figure 9 depicts the elastic properties determined for the well. As it can be seen using the procedure explained above, the ranges between generated static young modulus (E_ static) and experimental data from core analysis (E_ static core) have a reasonable match. It should be noted that the whole core samples were taken in the reservoir section which is below 3700 m MD.

Figure 10 shows the static Poisson's ratio for the well. The results show good match with the Poisson's ratio coming from triaxial compression tests. Since these magnitudes are calculated from the compressional slowness, shear slowness and bulk density, any artifact in well could cause some spike in the original log data that could consequently result in spike or some sharp trend in the calculated logs. This is a normal procedure in petrophysical evaluation and logging. It should be noted that these spikes and artifacts are not used in the final model were the investigation of under

balanced drilling will be conducted. The section for this matter will be cross checked to ensure that this artifact will have infinitesimal effect in the final model.

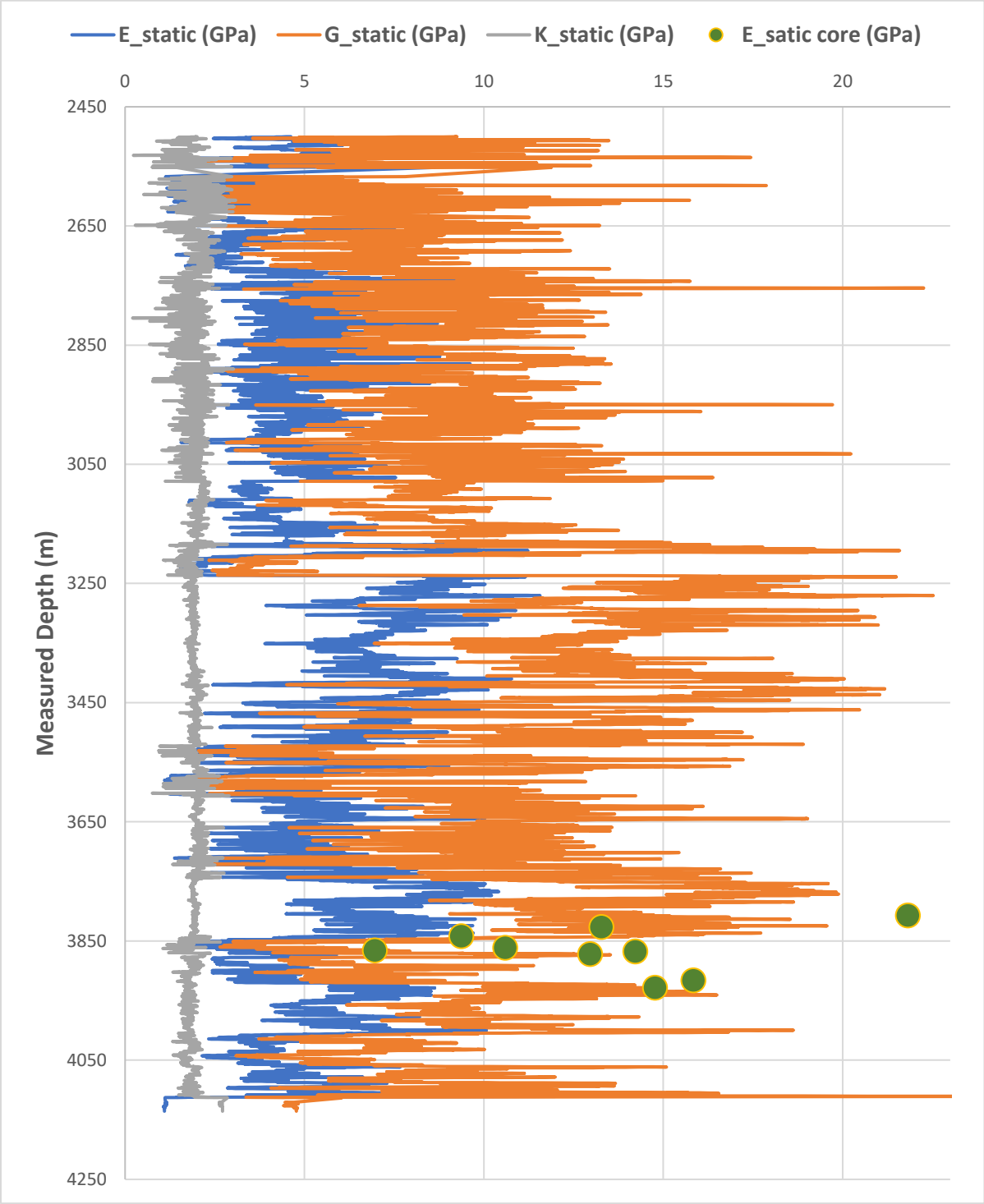

Figure 9 Elastic properties determined for the well.

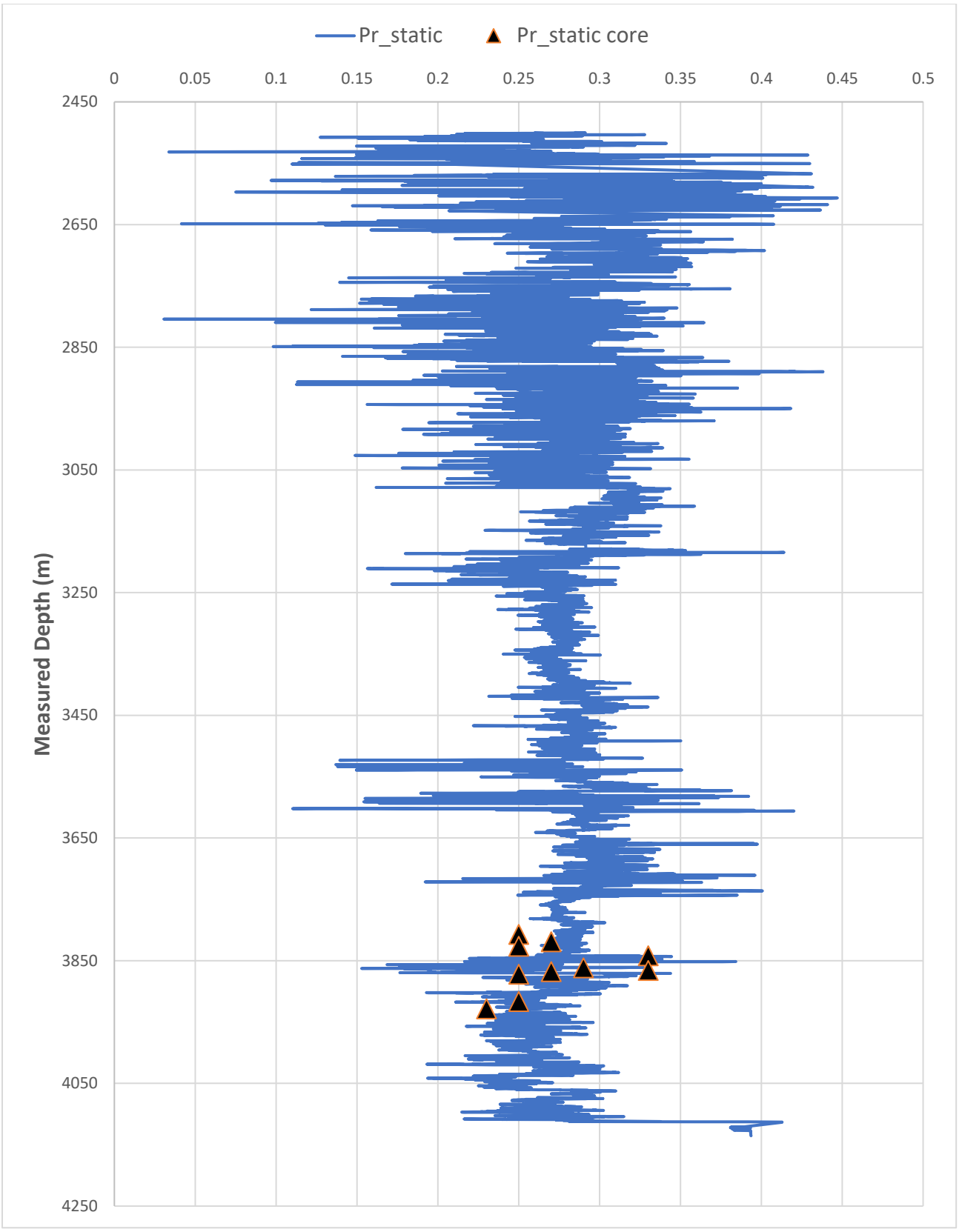

Figure 10 Static Poisson's ratio for the well.

2.5. Rock strength

Rock strength refers to the ability of the rock to withstand the in-situ stress environment around the wellbore. Unconfined compressive strength (UCS) is one of the most used rock strength parameters. UCS is typically computed from log measurements. Unconfined compression tests or multi-stage triaxial compression tests on cores provide a method for punctual calibration of the continuous log.

Several empirical equations are available for calculating UCS from log data. Most of them use rock elastic moduli (Young's modulus, shear modulus), porosity and other formation properties. To calculate UCS in the current study, a correlation was established between UCS and Young's modulus values from cores. This correlation is shown in Figure 11. The calculated and core derived values have been compared in Table 8.

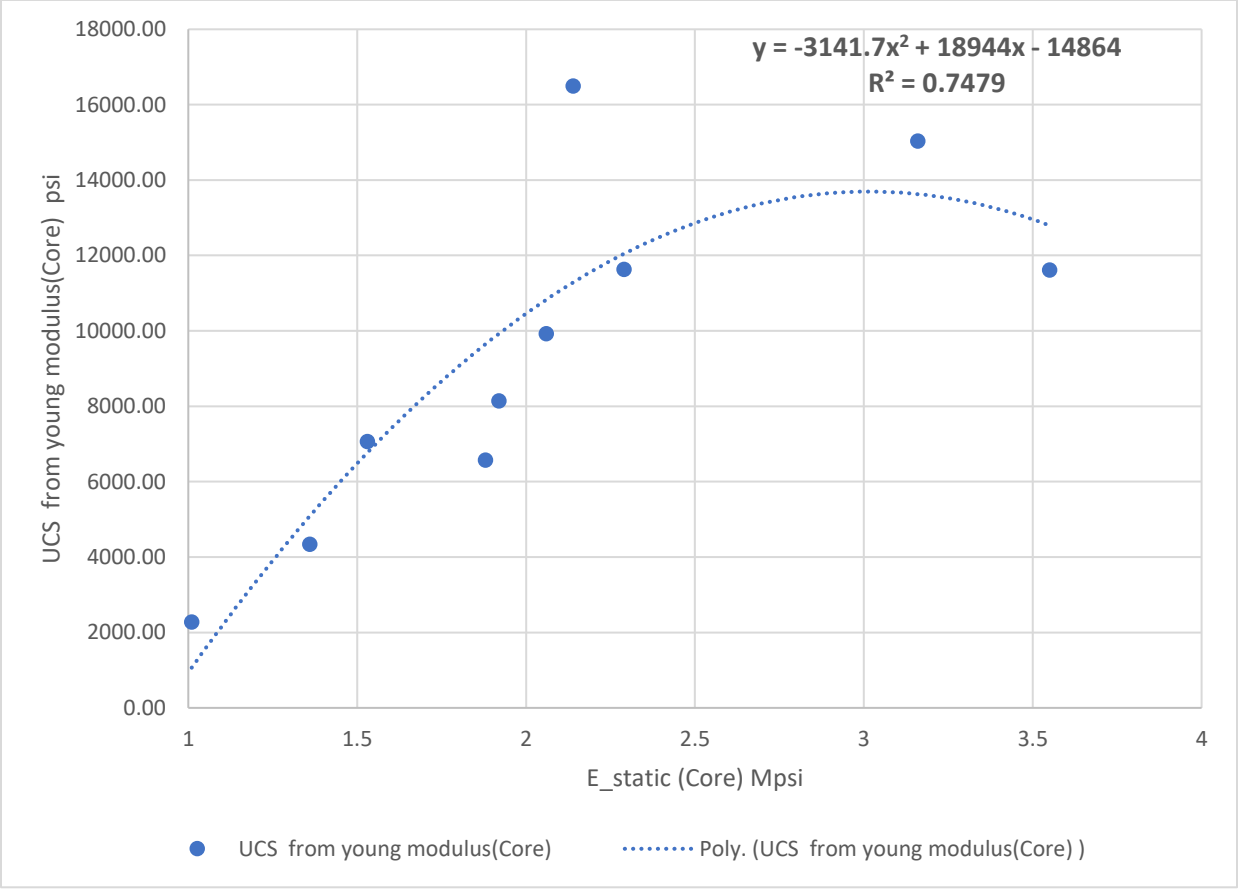

Figure 11 Correlation between UCS and static Young's Modulus for well.

Table 8 Comparing core derived and calculated values of UCS for well.

E_static (Core)	UCS from young modulus (Core)	UCS (Calculated)
Mpsi	psi	psi
3.16	15030.26	13627.28
3.55	11611.72	12793.93
1.92	8142.42	9926.92
1.36	4336.63	5088.95
1.53	7064.79	6765.91
1.01	2278.54	1064.59
2.06	9920.58	10828.52
1.88	6568.76	9646.70
2.29	11630.58	12042.37
2.14	16495.14	11288.43

The tensile strength of the formation was used to evaluate the tensile failure of the wellbore due to stress concentration. Since tensile strength (TSTR) of a rock is usually in the order of 1/12 to 1/8 of its UCS, and in lack of any other data for carbonates and/or shales, the tensile strengths of the rocks were assumed to be 1/10 of their UCS values. The calculated rock tensile strength was then calibrated using tensile strength (Brazilian) test's results (Table 9).

Table 9 Comparing core derived and calculated values of TSTR for well.

TSTR (Core) psi	TSTR (Calculated) psi
1638.926	1352.482
1037.02	1328.47
931.1423	860
916.6385	539.96
540.9908	493.84
581.6013	520.4
542.4411	520.3944
744.0436	745
1473.583	1244.12
977.5544	1005

As it can be seen from Figure 12, both the computed tensile strength and UCS show a promising match with the core results from laboratory tests.

Regarding the angle of friction, the results of mechanical tests on rocks were used and the calculated values are shown in Figure 13.

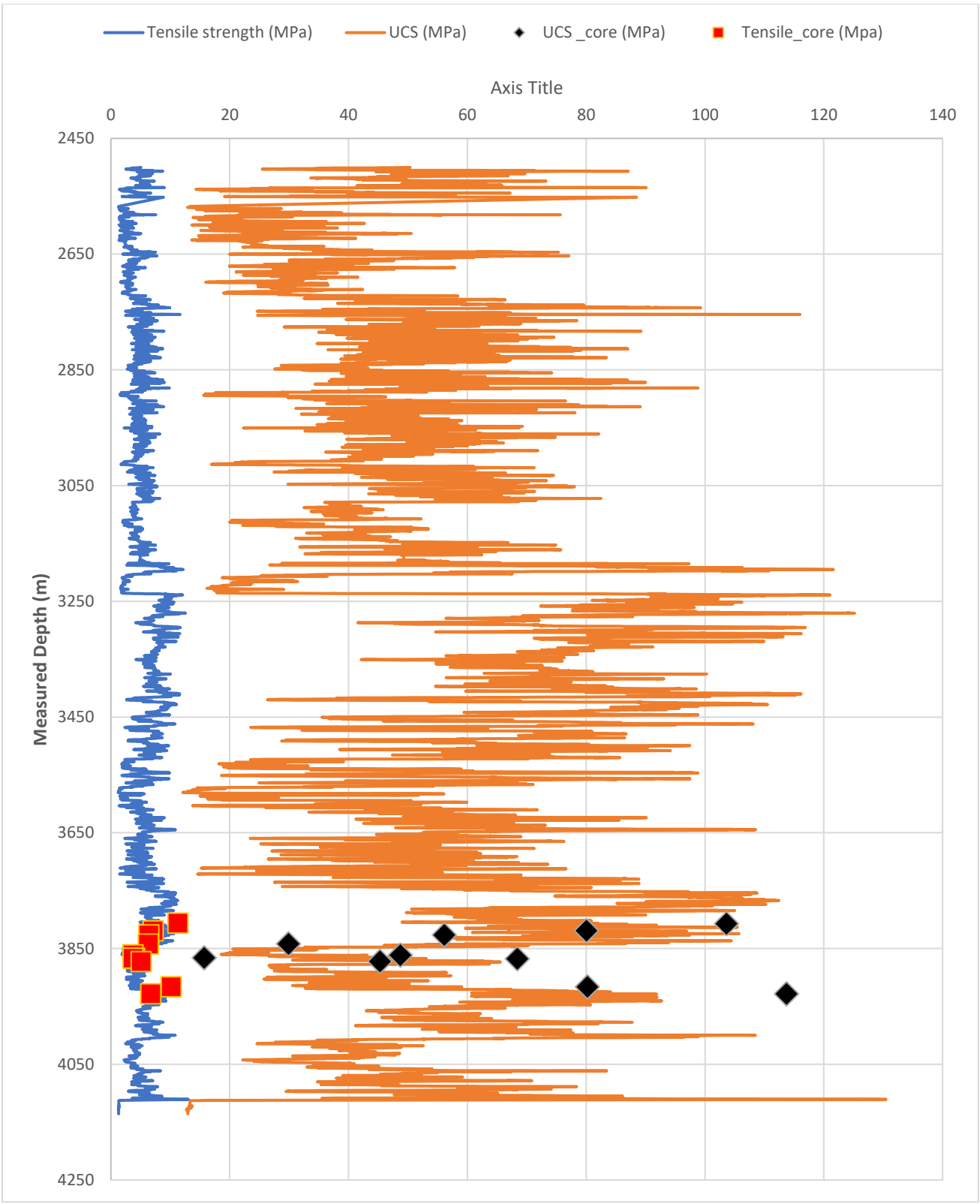

Figure 12 Tensile strength and UCS computed, and core results for the well.

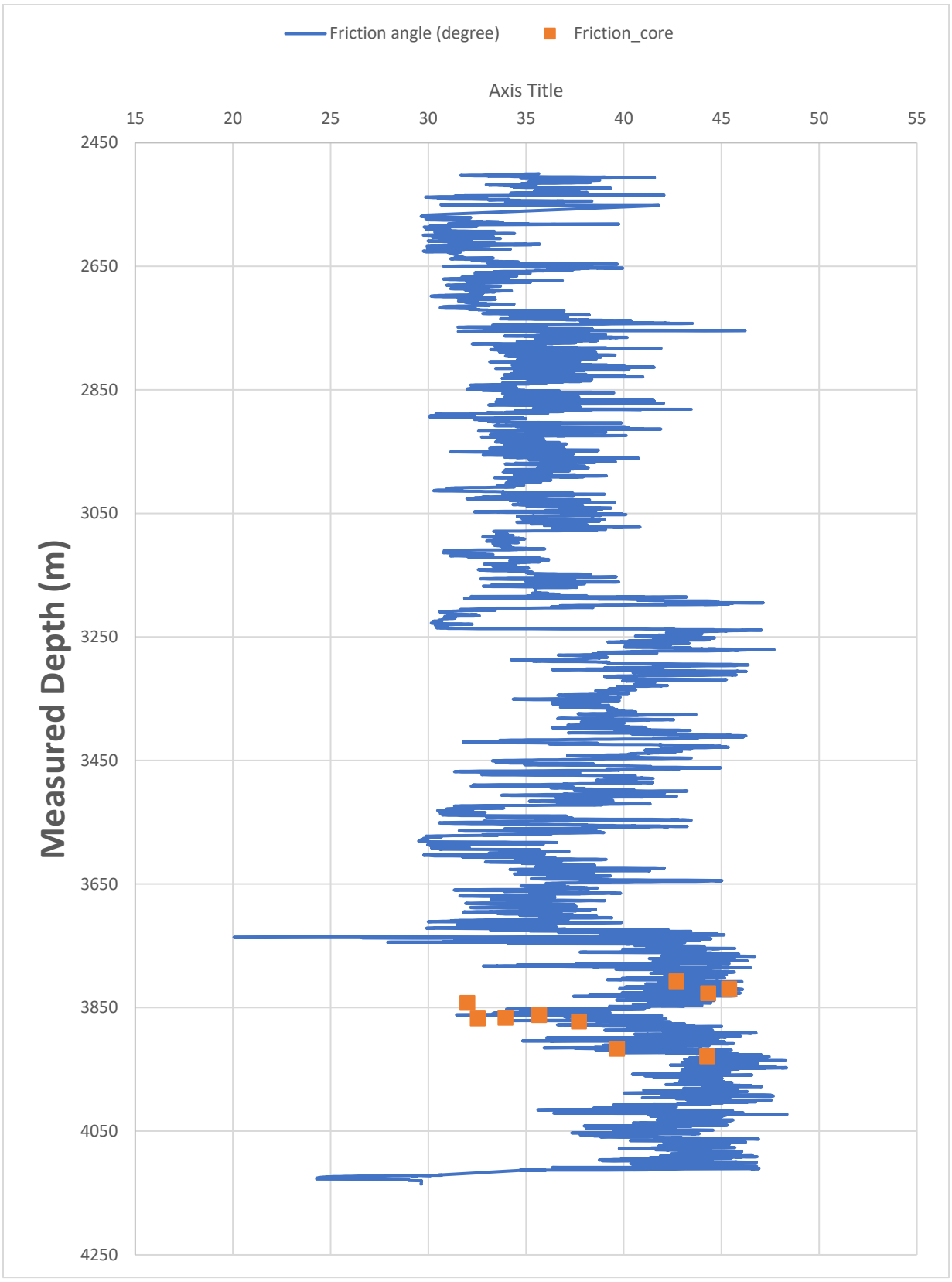

Figure 13 friction angle computed, and core results for the well.

2.6. Vertical stress

The vertical stress σ_v was calculated by integrating the bulk density of the formation ρ_b from the surface to TD, using the following equation:

Equation 7 $\sigma_v = \int_0^z \rho_b(z).gdz$ *Vertical stress*

For the intervals of missing or poor log quality, the rock density has been extrapolated using the equation below:

Equation 8 $\rho_b = \rho_{sur} + A_0 .(TVD - WD - AG)^{\alpha}$ *Density extrapolation*

where:

ρ_b: Formation density

ρ_{sur}: Formation density at surface or seabed

TVD: True Vertical Depth, m

WD: Water Depth, m

AG: Air Gap, m

A0, alpha: Extrapolation parameters

Figure 14 shows the vertical stress calculated by integrating the composite density log.

2.7. Pore pressure

Pore pressure is a crucial component in a Mechanical Earth Model, particularly for stresses and wellbore stability analysis. Sonic or resistivity logs are commonly used to identify pore pressure trends in shale and to calculate pore pressures. However, the produced formation pressure must be calibrated against actual pore pressure measurements. Pore pressure may also be computed using constant pressure gradients that can be determined from pressure measurements, when available.

There are various methodologies for calculating pore pressure using log data, most of them being effective stress-based approaches. Examples include the frequently used Eaton Method (Eaton 1975), Equivalent Depth Method (Foster 1966), Bowers method (Bowers 1995), etc.

Most effective stress pore pressure prediction methods consist of three steps:

1. The overburden stress is determined from measured or estimated bulk density data.
2. The vertical effective stress is estimated from a pore pressure indicator measurement, such as sonic slowness, seismic velocity, or resistivity.
3. The pore pressure is obtained from the difference of 1 and 2.

In the current study, since resistivity log is available only for reservoir section, sonic log has been used to calculate pore pressure of non-reservoir section for the mentioned well. The reservoir section pressure gradient from MDT and XPT tools were used. The final pore pressure profile was calibrated against the weight of the applied mud used for drilling the well. In some intervals, due to lack of shale layers, the computed pore pressure is not robust and calibrated with respect to the weight of the applied mud. Figure 14 depicts the results of the procedure explained above.

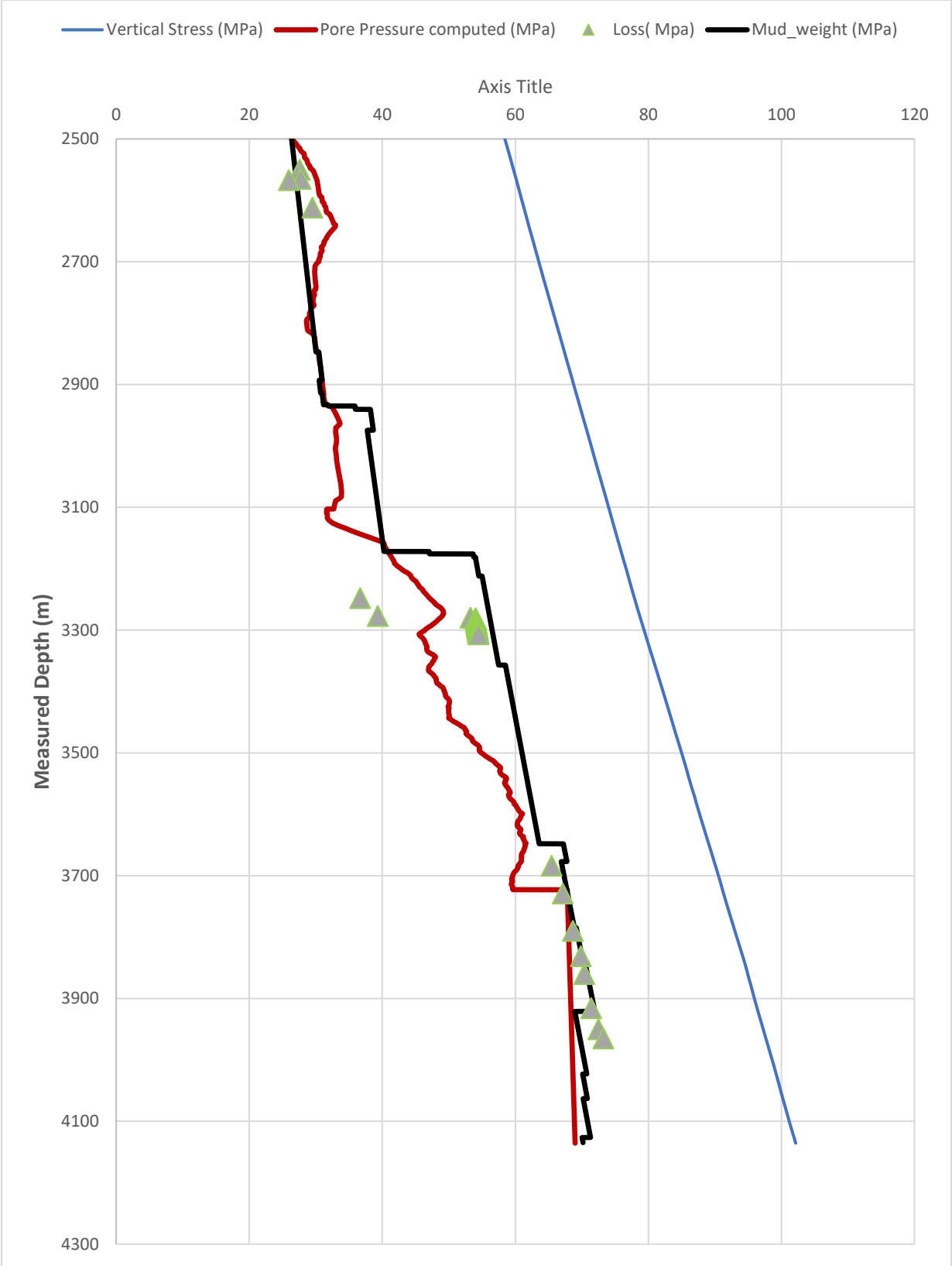

Figure 14 Vertical stress, computed pore pressure calibrated with mud weight in well and drilling events (MPa).

2.8. Horizontal stress magnitude

Stress magnitudes, including those of in-situ stresses in rock, cannot be explicitly measured but can only be modeled or inferred from other measurements of deformation, strain, pressure, etc. However, there is a number of fundamental conditions that must be honored, and which constrain the magnitudes and directions of principal stresses σ_1, σ_2, and σ_3 in a solid body (including those stresses in the ground).

For instance, at a free surface (i.e., ground surface) or at the surface of a body that cannot sustain deviatoric stresses (i.e., the stress state is isotropic), shear stresses (τ) must be zero, and therefore the principal stresses must be aligned parallel and perpendicular to the surface.

Similarly, principal stresses must be near parallel and near perpendicular to any plane unable to sustain high shear tractions (i.e., weak faults). Therefore, other than in close proximity to faults, salt diapirs, mud volcanoes or near-surface in mountainous areas having greater topographic contrast (Ali 2003), or where the stress state is perturbed by significant heterogeneous depletion or local injection, the natural state of stress in otherwise shallow sedimentary basins is usually one where the minimum in-situ horizontal stress σ_h, the maximum in-situ horizontal stress σ_H and the overburden stress σ_V are the principal stresses. However, the order of these stresses can vary, as represented by the three Andersonian-type fault models (Anderson 1905).

The magnitudes of these principal stresses are further constrained (but not uniquely defined) by those magnitudes of the horizontal stresses that, together with overburden stress and pore pressure, satisfy conditions of limit-state corresponding to some appropriate rock-failure criterion. For instance, in the case of a linear Mohr-Coulomb peak strength criterion being applicable, the lower bound value for the effective minimum in-situ stress σ'_3 and the upper bound value of the effective maximum in-situ stress σ'_1 are related to one another by the following equation, where UCS is the unconfined compressive strength and ϕ is its internal friction angle:

Equation 9 $\acute{\sigma_1} = UCS + \acute{\sigma_3}\left(\frac{1+sin(\phi)}{1-sin(\phi)}\right)$ *Mohr-Coulomb constraint to stresses*

Of the two horizontal stresses, the magnitude of σ_h is more straightforward to determine if it happens to be the in-situ minimum stress σ_3 and is therefore less than the overburden stress. With mini-frac or extended leak-off test indirect measurements of σ_3 (and therefore σ_h) can be obtained with reasonable accuracy. However, the magnitude of the maximum horizontal stress σ_H is more difficult to determine, and it is best quantified by an integrated approach that applies the above-mentioned constraints together with some appropriate modeling, and involves rigorous calibration to observed features, such as wellbore breakout or drilling-induced tensile fractures.

In a passive basin, if the rock can be assumed to be a semi-infinite isotropic medium subjected to gravitational loading and no horizontal strain, the two horizontal stresses are equal in magnitude. They can be estimated (Plumb, Krabbe et al. 1999) from pore pressure P_P, overburden stress σ_V, Biot's coefficient and static Poisson's ratio using the following uniaxial strain poro-elastic equation:

Equation 10 $\sigma_h = \frac{\nu}{1-\nu}(\sigma_v - \alpha P_p) + \alpha P_p$ *Horizontal stresses in a passive basin*

In a tectonically active basin, stresses and strains arise from tectonic plate movement. If tectonic strains are applied to rock formations, they add a stress component in an elastic rock. The poro-elastic horizontal strain model (Blanton and Olson 1999) takes tectonic strains into account, and therefore accommodates anisotropic horizontal stresses.

Equation 11 $\sigma_h = \frac{\nu}{1-\nu}\sigma_v + \frac{1-2\nu}{1-\nu}\alpha P_p + \frac{E}{1-\nu^2}\varepsilon_x + \frac{\nu E}{1-\nu^2}\varepsilon_y$ *Poro-elastic horizontal strain model for* σ_h

Equation 12 $\sigma_H = \frac{\nu}{1-\nu}\sigma_v + \frac{1-2\nu}{1-\nu}\alpha P_p + \frac{E}{1-\nu^2}\varepsilon_y + \frac{\nu E}{1-\nu^2}\varepsilon_x$ *Poro-elastic horizontal strain model for* σ_H

Here the two horizontal strains ε_x and ε_y may be compressional (for tectonic compression) or extensional (i.e., to represent lateral spreading), and can be treated simply as calibration factors that can be adjusted to best match the stress estimates to minimum horizontal stress measurement or specific modes of rock failure seen on image logs etc.

The model can be applied without making any pre-assumptions about the stress regime (other than the horizontal and vertical stresses are the principal stresses) or about the order of the horizontal

and vertical stresses. Instead, these details and information come from calibrating the model using data from the well and drilling data, etc.

Therefore, the most rigorous process available for estimating the complete state of in-situ stress in the ground (magnitudes, order and directions) at a single well location, and particularly to determine the magnitude of σ_H, involves some initial estimate of the range of possible stresses, as constrained by limit state or other mechanics considerations, and subsequently constrained and refined to generate a more specific prediction. The horizontal stresses are further calibrated and validated using all available information to achieve a final model that is consistent with all the stress indicators. The used values for ε_x and $\varepsilon_y$in this study were respectively 0.1 and 0.9.

Figure 15 shows the stress profile for well. Minimum horizontal stress, maximum horizontal stress, overburden stress and pore pressure are depicted. The stress model indicates that the stress regime in the interval under study is normal ($\sigma_v > \sigma_H > \sigma_h$) toward strike-slip ($\sigma_H > \sigma_v > \sigma_h$).

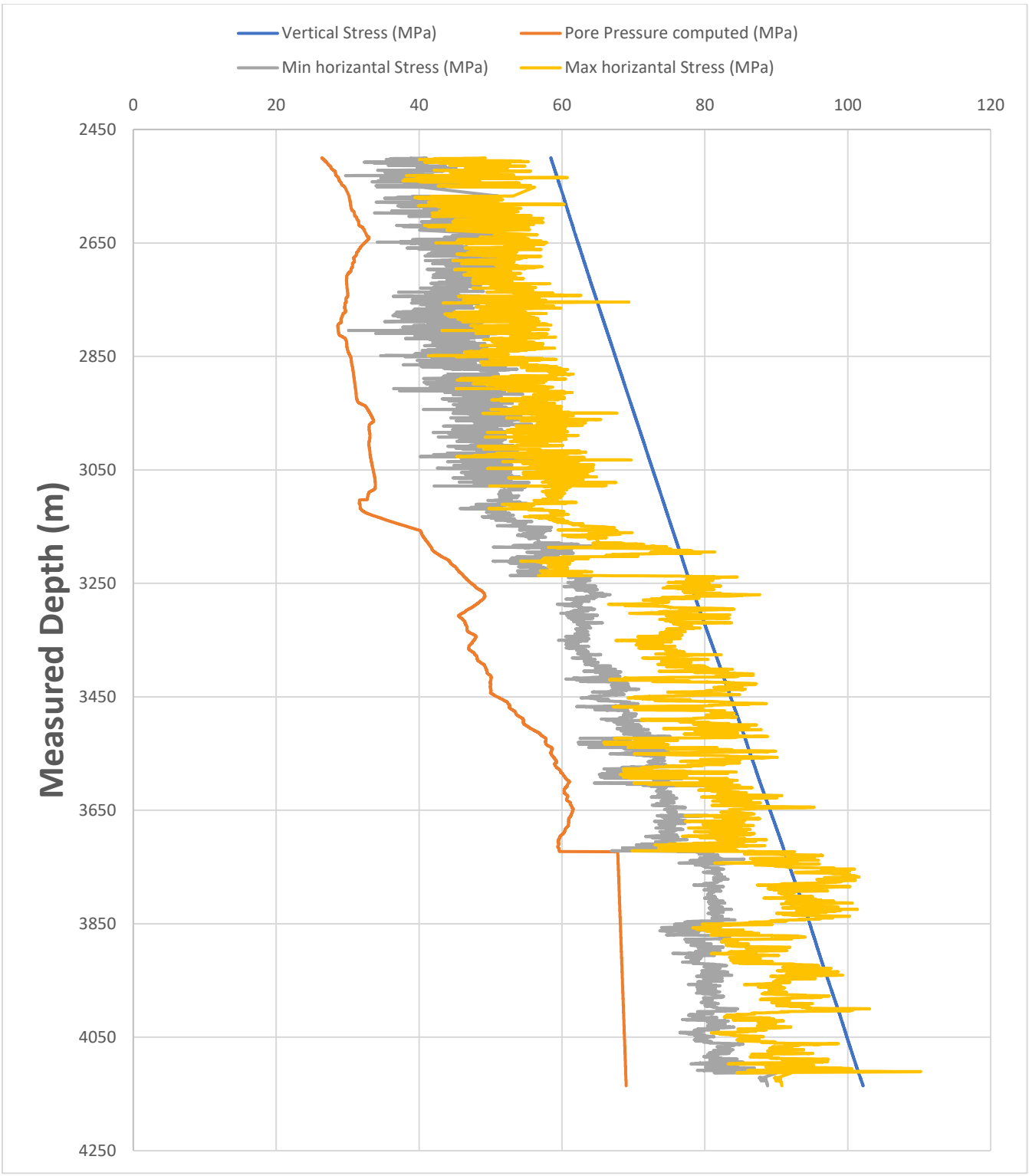

Figure 15 stress profile for well, Minimum horizontal stress, maximum horizontal stress and overburden stress and pore pressure.

2.9. Mud weight window

The most effective approach to calibrate and validate the MEM is to verify the predictability of the model. Using the estimated rock properties and horizontal stresses, wellbore stability analysis will show how robust the MEM is by comparing the predicted wellbore stability/instability with the drilling event, image, caliper etc.

Wellbore instability due to rock failure is caused by two major types of failure, tensile or shear. Shear failure is usually caused by low mud weight, whereas tensile failure is caused by high mud weight. Several methods exist for predicting rock failure (and wellbore instability). The most commonly used failure criteria include the Mohr Coulomb to determine the shear failure, and Maximum Tensile Stress to determine the tensile failure.

One of the outputs of the wellbore stability analysis is a mud weight window. Figure 16 shows the concept of the mud weight window.

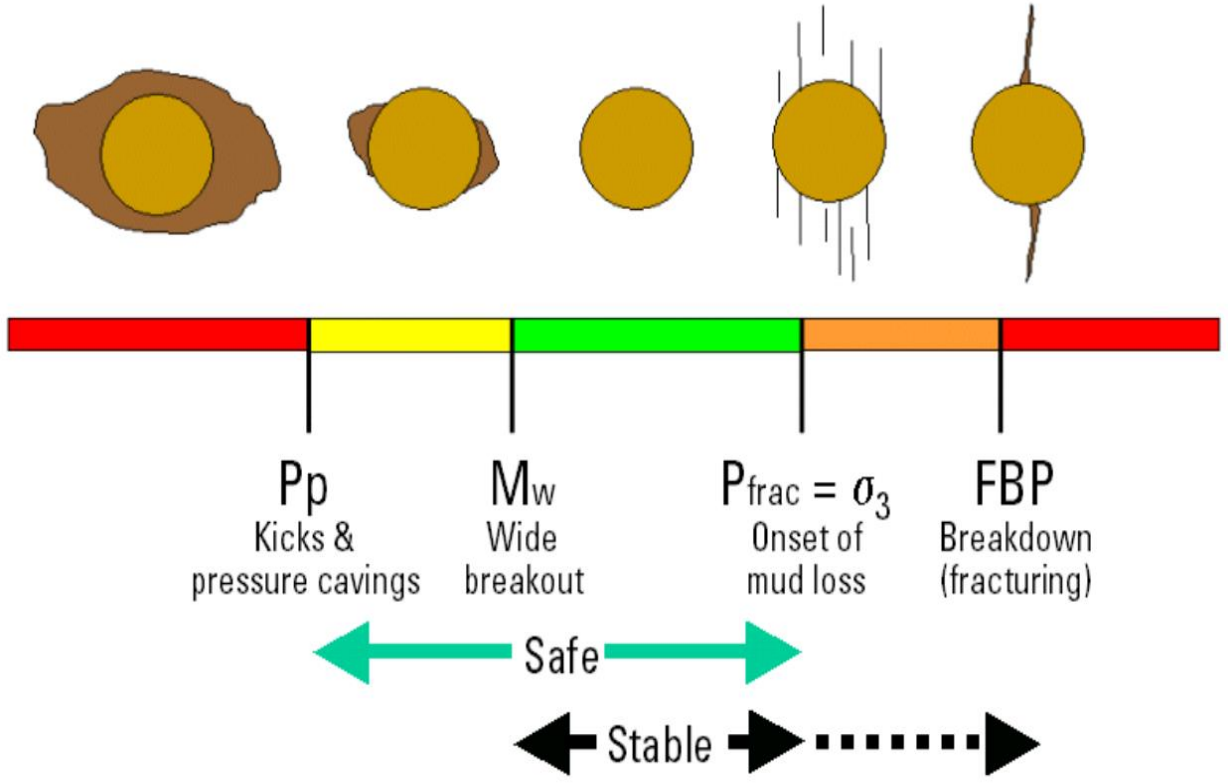

Figure 16 The mud weight window concept (Pašić, Gaurina Međimurec et al. 2007).

There are four critical values in defining the mud weight window:

1. **Pore pressure (Pp)** - If mud weight (wellbore pressure) is less than pore pressure during drilling, pressure carvings, wellbore washout, and/or kicks might be expected.
2. **Minimum mud weight (Mw) for preventing breakout** - Below this mud weight, rock failure and therefore wellbore breakout is likely to occur. The lower the mud weight below this value, the more severe the breakout will be. Swabbing, that might reduce the instantaneous hole pressure below this equivalent mud weight, can have a similar effect.
3. **Minimum in situ stress (σ3)** - If natural fractures or any other conductive fissures exist around the wellbore, or in presence of a highly permeable zone, then mud weight above the minimum in situ stress (known in drilling as fracture pressure Pfrac) will tend to re-open the natural fractures and causing loss of drilling fluid to the formation.
4. **Formation breakdown pressure (FBP)** - When the mud pressure is higher than the formation breakdown pressure, tensile failure can occur in the intact rock and hydraulic fractures will be induced in the wellbore wall. If this breakdown pressure exceeds the minimum in situ stress σ_3, total losses may occur, as the pressure in the well reaches this value.

However, whilst the above critical values are illustrated in Figure 16 in that specific order, the order can be different, depending on the stress regimes and wellbore geometries. For instance, the minimum mud weight for preventing breakout can be lower than the pore pressure, and the minimum horizontal stress can be higher than the formation breakdown pressure. In some cases, the minimum horizontal stress or the formation breakdown pressure can be lower than the minimum mud weight for preventing breakout, and this is the case where stable mud weight window doesn't exist.

Whatever the order, it can be seen that an ideal mud weight would be higher than the pore pressure and the minimum mud weight for preventing breakout, but lower than the minimum horizontal stress and formation breakdown pressure (both safe and stable).

Figure 17 shows the calculated mud weight window for the well using the data provided by the MEM built and calibrated with the drilling event and the data provided by test results and MDT. For better visualization the logs were shown using the petrel software

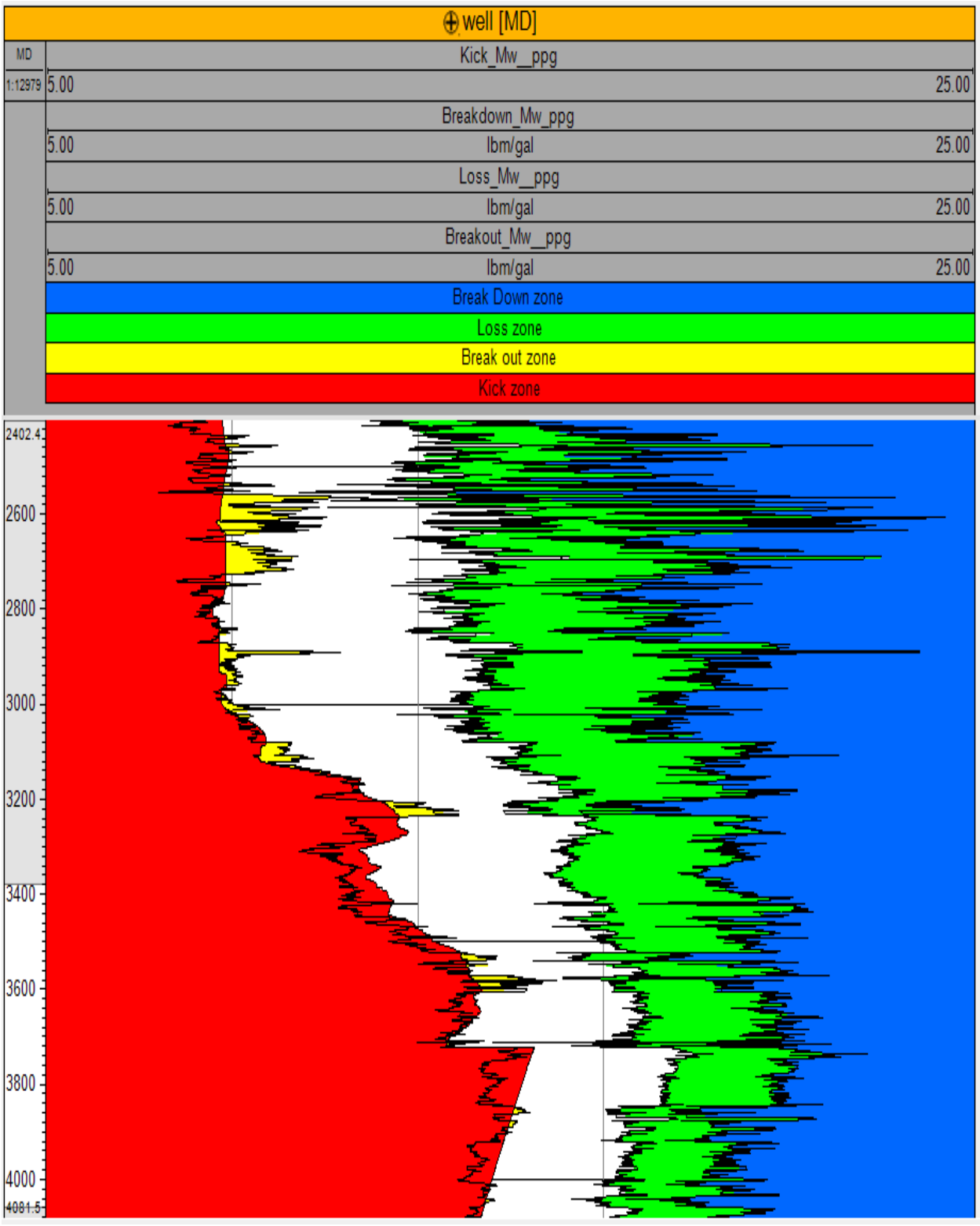

Figure 17 computed mud weight window for the well ppg.

Drilling mud fulfils a number of important roles during the drilling process. It cools the drill bit, transports cuttings to the surface, keeps the wellbore mechanically stable and avoids an influx of fluids into the wellbore. Mud Weight Windows (MWW) enables the assessment of geomechanical drilling risks based on a geomechanical model. This assists in choosing the density of drilling mud (the "mud weight") to keep the well mechanically stable (avoid wellbore breakouts and creation of induced fractures) and avoid an influx of fluids.

1. **"Pore Pressure higher than the mud weight".** In this situation, the pressure of fluids (oil, gas or Water) in the rock formation is higher than the hydrostatic pressure (calculated from the density of the mud and the height of the column) in the wellbore. When drilling into a permeable formation or fracture, this leads to an influx of liquid into the wellbore. If this influx is strong, it is called a "kick", and in the worst case is a "blowout" (Red area in Figure 17).

2. **"Breakout"**. During drilling, the stress state in the wellbore wall is perturbed. These stress perturbations are due to replacing a cylinder of rock with a cylinder of fluid of a different density. For low mud weights, large differences in (far-field) principal stresses and low strength rock, the stress concentration in the near wellbore can lead to shear failure in the wellbore walls, creating breakouts. Large volumes of breakouts can result in catastrophic wellbore failure, causing "stuck pipe" events (Yellow area in Figure 17).

3. **"Fracture gradient"**. For high mud weights, the wellbore pressure can exceed the (far-field) minimum principal stress. In this case, an induced fracture will propagate into the formation, and mud losses can occur (Green area in Figure 17).

4. **"Breakdown"**. For high mud weights and large differences in (far-field) principal stresses, the hoop stress in the near-wellbore wall can become tensile. If the magnitude of the tensile hoop stress exceeds the tensile strength of the rock, a tensile fracture is induced in the wellbore wall. The mud weight (or mud density) at which drilling-induced fractures are first caused is called the breakdown mud weight (Blue area in Figure 17).

The mud weight Window (MWW) can then be defined as the allowable range of mud weights for a given drilling direction such that none of these four mechanisms (pore pressure larger than mud weight, the occurrence of breakouts, breakdown, or mud weight exceeds fracture gradient) is triggered.

Figure 18 represents the mud weight magnitude in ppg. This value can be computed by subtracting the maximum value between the breakout and kick minus the minimum value between the loss and break down. A large positive mud weight window indicates a low risk of geomechanical difficulties while drilling with an appropriate mud weight. A negative mud weight window can also occur. In such cases, drilling a well may still be possible. For example, by drilling with a low-density mud, wellbore breakouts may occur or there could be an influx of formation fluid into the wellbore. These conditions would be managed by the drilling engineer (close to 2550m, 2650 m, and 2800 m of measured depth).

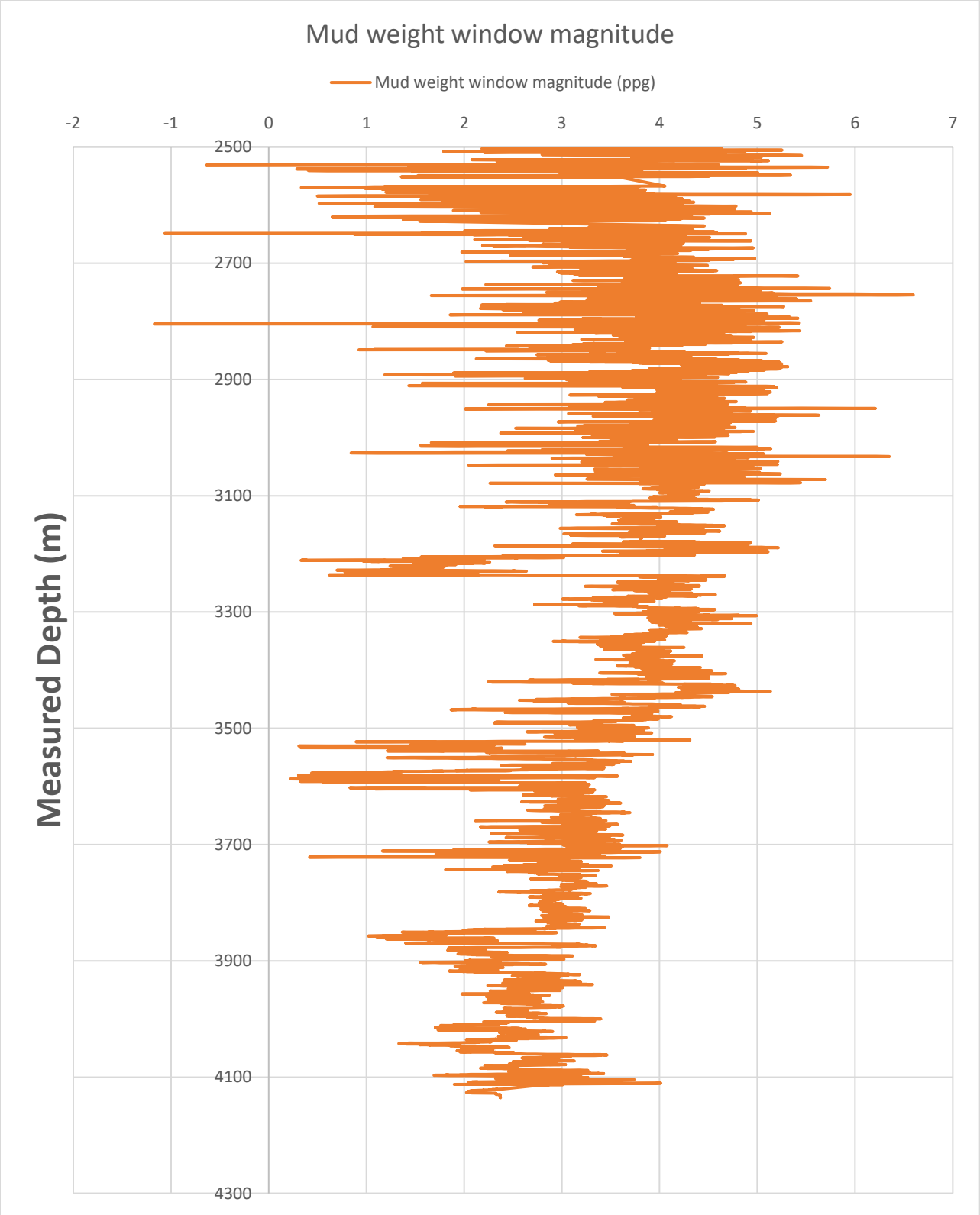

Figure 18 Mud weight window magnitude ppg.

3. UBD feasibility

3.1. Methodology

It has been reported in the literature that rock formations could withstand higher stresses than the estimated strength of the formation itself, due to the plastic behavior of borehole rock (McLellan, Hawkes et al. 2000, Hareland and Dehkordi 2007, Rahman, Khaksar et al. 2010, Salehi, Hareland et al. 2010, Kim and Sharma 2012, Khatibi, Aghajanpour et al. 2018, Khatibi, Farzay et al. 2018). In addition to the plastic deformation that could be allowed in the fields, the higher holding of stresses in the fields could be also achieved due to the application of the conservative Mohr-Coulomb criterion in the studies(Al-Ajmi and Zimmerman 2005, Al-Ajmi and Zimmerman 2009). In wellbore stability modeling, the level of stress concentration around a borehole is a function of borehole pressure: if it is lower than the formation pore pressure, then the borehole could be safely drilled with the application of UBD technique.

To determine the critical application that will initiate wellbore instability, NYZA is utilized as a criterion (Figure 19). Experimentally, vertical wellbores encounter instability challenges when NYZA value is greater than 1.0 (McLellan, Hawkes et al. 2000). The critical limit of NYZA could increase to 1.2 or even be higher when considering well deviation, operation settings, and hole cleaning capacity(McLellan 1996, McLellan, Hawkes et al. 2000).

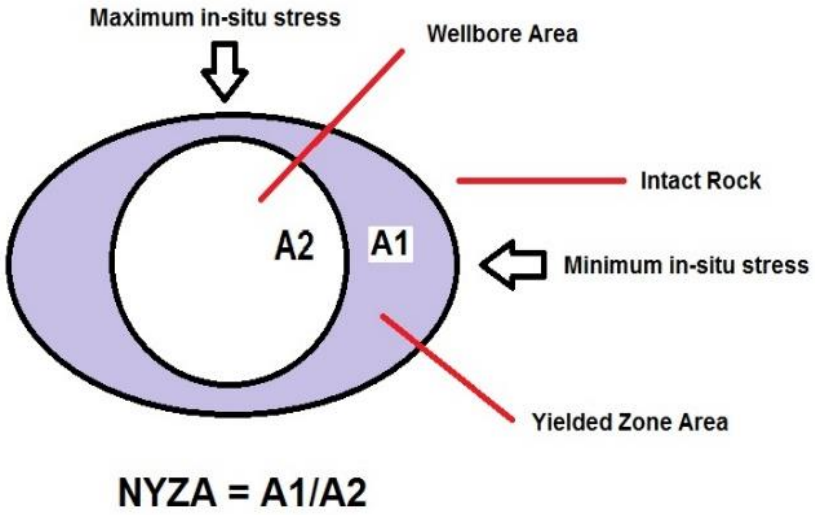

Figure 19 The cross-sectional area of the yielded rock around the wellbore divided by the area of the original wellbore (NYZA).

In the finite explicit simulator, as the first step, in situ stresses, pore pressure and rock properties were added to the model. The developed model was then run to reach initial equilibrium where the formation has not been drilled yet. Afterward, the null model and the mud weight were introduced to model the drilling of the formation and stabilize the open hole section for a vertical well. When the model reached equilibrium, the plastic area around the wellbore was calculated by a fish code that was written for computing NYZA in FLAC 3D. Each studied mud weight will result in a different NYZA and displacements around the wellbore. After that, the NYZA values and their associated mud weights were plotted, and the best curve was fitted to the results as shown in

Figure 20. The mud weight corresponding to NYZA value equal to 1 is considered as the optimum mud weight, that is the minimum mud weight required to stabilize the wellbore. If the optimum mud weight obtained is less than pore pressure, then UBD operation can be implemented to drill vertical wells in the field. The flowchart of this modeling methodology is illustrated in Figure 21.

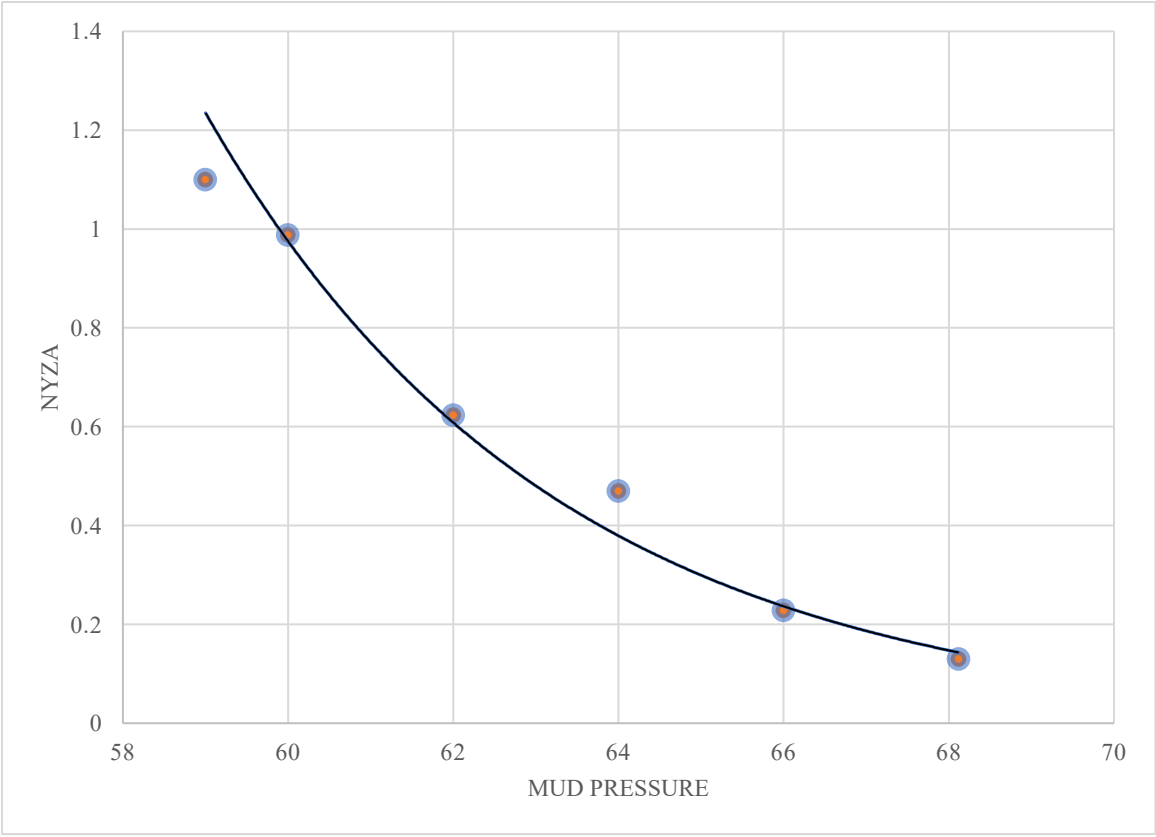

Figure 20 Changes in NYZA by increasing the mud weight (MPa).

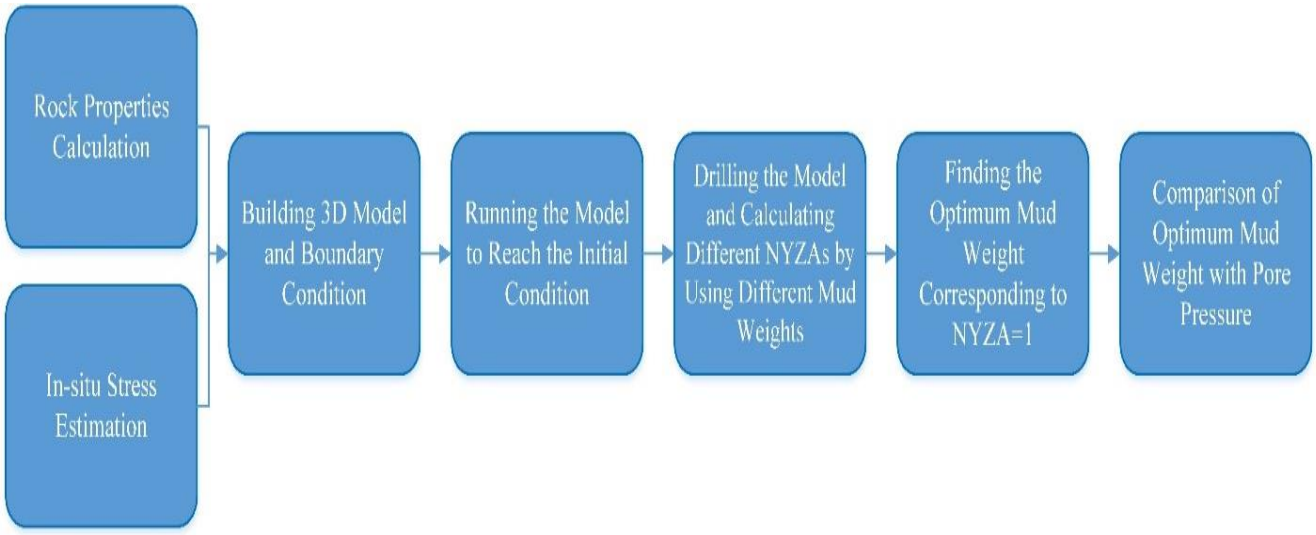

Figure 21 Flowchart of finding optimum mud weight using NYZA criterion in FLAC 3D.

In this study, the NYZA function is written in fish language within the FLAC 3D software by gathering the volume of any plastic zone around the wellbore which was affected by drilling the well. The NYZA value is then calculated through the following equation(McLellan, Hawkes et al. 2000):

$$NYZA = \frac{P}{(H*\pi*r^2)} \qquad \textit{Equation 13}$$ *NYZA Equation*

where P is a cumulative volume of all plastic zones around the wellbore, H is the drilled depth or model height and r is the well radius.

3.2. Modelling development

In the modelling process, each model size was extended about 10 times of the well radius to be sufficient for eliminating the artifacts caused by end-effects in stress distribution. Moreover, grids are designed to be smaller as they get closer to the wellbore to increase the accuracy of plastic zone and displacement calculation around it. With respect to effective stresses around borehole, Kirsch solution was applied to validate the mesh. Then, boundary conditions were assigned into the model and a failure criterion was used to simulate the plastic strains outputs. As shown in Figure 22, velocity values and unbalanced forces converged to zero as the run number increased in each step, which indicates that the model has reached the equilibrium (Capasso and Musso 2010, Alquwizani 2013).

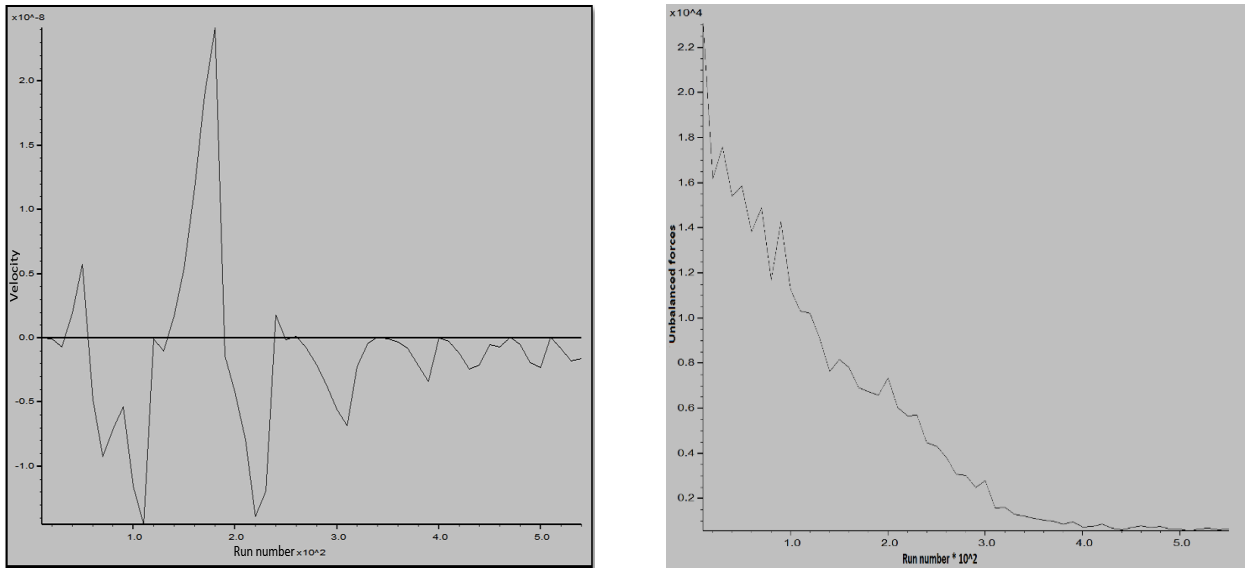

a) b)

Figure 22 (a)Velocity and (b) unbalanced force vs. run numbers.

The modeling was completed for five depth intervals in the reservoir section. Each model has a size of 2 m x 2 m x 4 m, which is laterally 10 times the well radius. Due to the small wellbore diameter in the reservoir section, the grids are designed to decrease approaching the well by a ratio of $3/4$. The model was created for each depth range and the geometry of the model, along with the magnitude of the minimum principal stress, is shown in Figure 23. In addition, the following field data are extracted from the 1D MEM of the well that was computed in the previous chapter, for the purposes of use in that model:

- Poisson's Ratio (v)
- Shear Modulus (μ)
- Friction angle ($\emptyset$)
- Bulk Modulus (K)
- Cohesion (C)
- Young's Modulus(E)
- Pore pressure (Pp)
- Vertical stress (Sv)
- Maximum horizontal stress ($SHmax$)
- Minimum horizontal stress ($Shmin$)

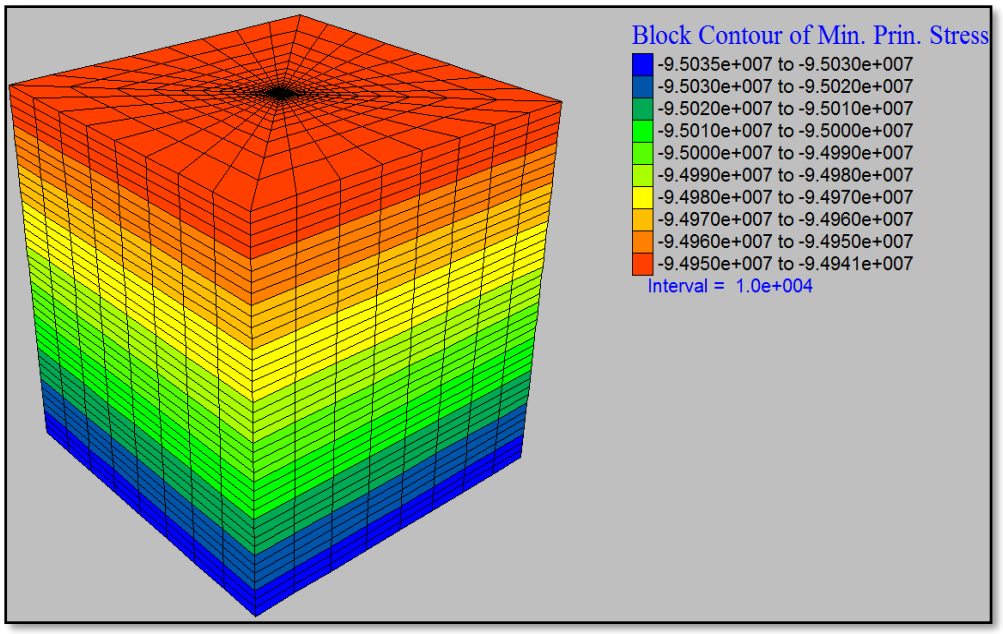

Figure 23 Model geometry with 2mx2mx4m dimensions along with minimum principal stress (MPa).

In the model, each height of 4 m has the same rock properties for all grids. For stress gradients, however, the model considers the stress variation by depth along the block. In this case study, the stress regime is initially a strike-slip (i.e., $S_{Hmax} > S_v > S_{hmin}$) at a depth of 3807 m; then, it changes to a normal fault stress regime (i.e., $S_v > S_{Hmax} > S_{hmin}$) up to the end of the modelled depth at 4040 m.

3.3. Model analysis

The model for each depth interval was run with three different mud weight categories. One mud weight category was kept lower than the pore pressure, the second mud weight category was designed higher than the pore pressure and the third one was adjusted to be approximately equal to the pore pressure. For the applied mud weights, the wellbore plastic zones were evaluated for the stability analysis. For instance, Figure 24 shows the plastic zone around the wellbore at an interval of 3861-3865 m created at different mud weights. (shear-p, tension-p) are the result of initial plastic flow that occurred at the beginning of the simulation. Subsequent stress redistribution has unloaded the yielding elements so that their stresses no longer satisfy the yield criterion. Only actively yielding elements (shear-n, tension-n) are important to the detection of a failure mechanism.

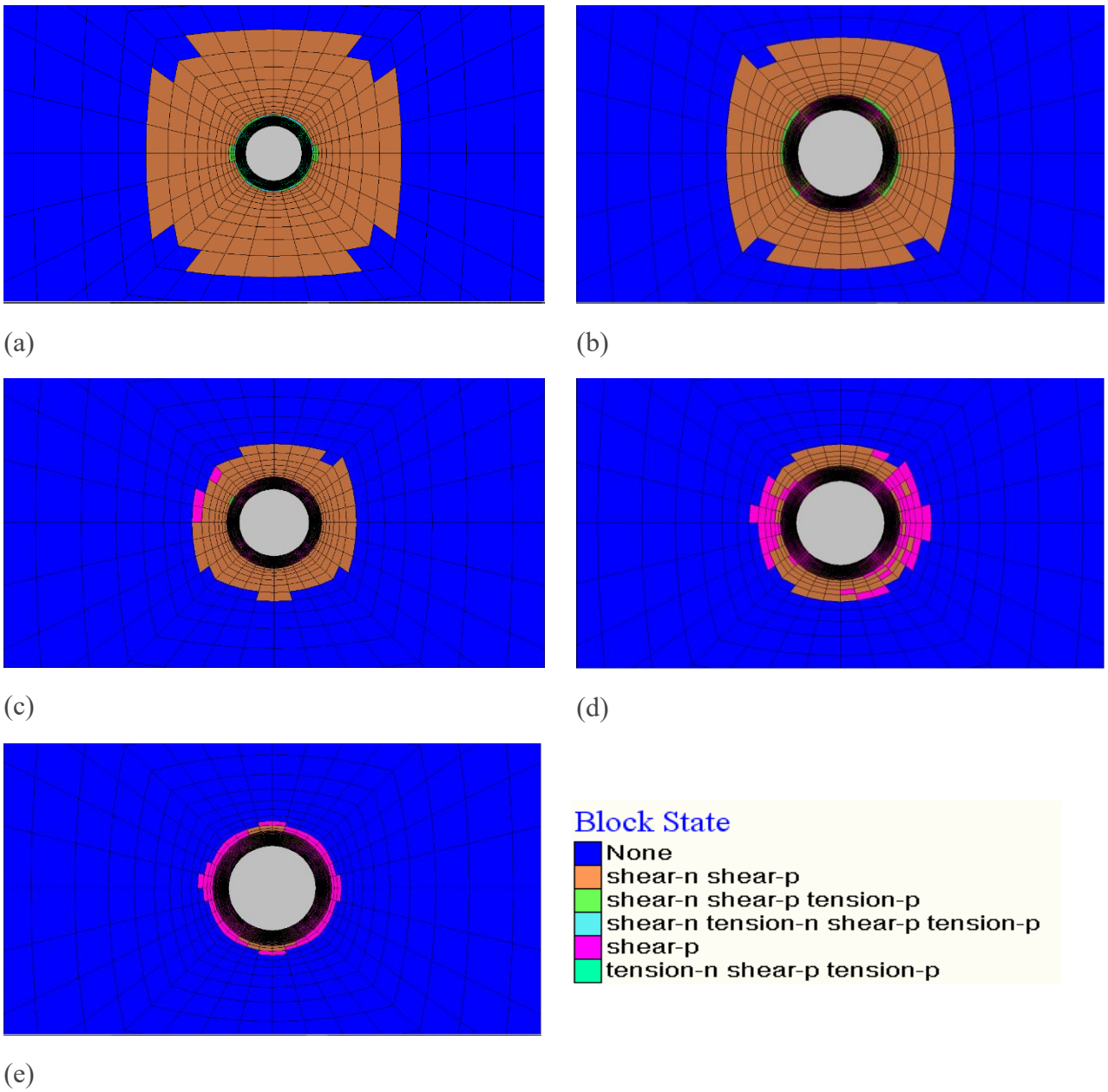

Figure 24 Created plastic zone around the wellbore by applying different mud pressure for the interval 3861-3865. (a) Mud Pressure = 64 MPa, (b) Mud pressure = 66Mpa, (c) Mud pressure = 67.5 MPa, (d) Mud pressure = Pore pressure = 68.2 MPa, (e) Mud pressure = 71 MPa.

It can be clearly observed that the plastic zone area decreases by increasing the mud weight value. Furthermore, since horizontal stresses are not equal in magnitude due to stress anisotropy of the field, the plastic zone created is not symmetric, and the maximum plastic zone propagation is in the direction of the minimum horizontal stress (see Figure 25).

With respect to the maximum grid displacement, the values are estimated in the direction of minimum horizontal stress (S_{hmin}) and maximum horizontal stress (S_{Hmax}) of the field. At the depth range 3861-3865 m, for example, the grid displacements along the horizontal stresses for different mud pressures are recorded in Table 10. It can then be concluded that the maximum displacement occurs along the direction of the minimum horizontal stress. Furthermore, it was observed that the greater the anisotropy of the stresses, the greater the difference in displacements between the directions of the horizontal stresses; and, by increasing the pressure of the mud, the displacements are reduced. (Figure 26).

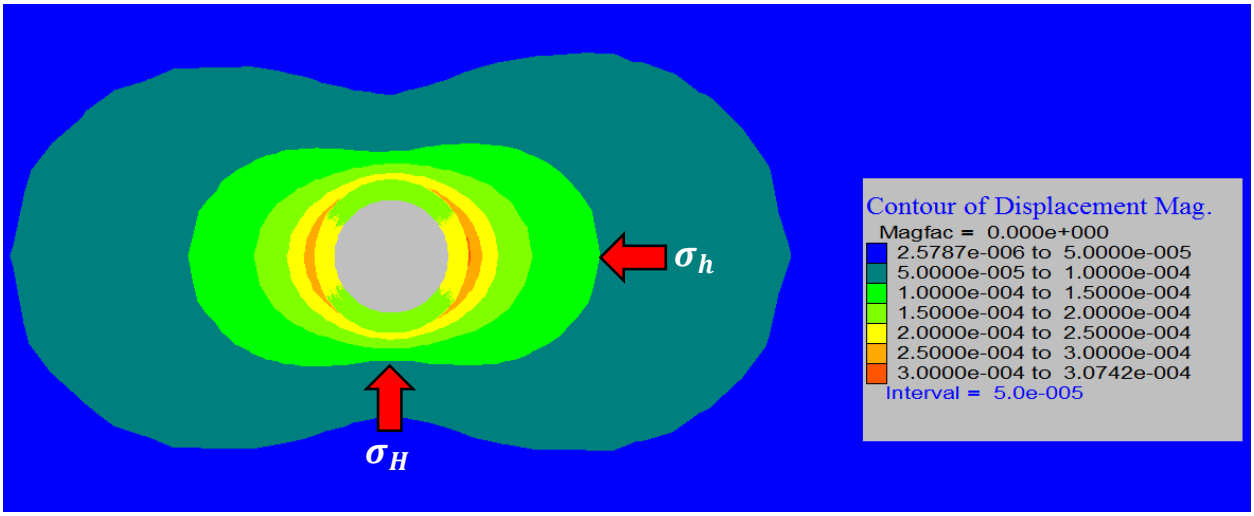

Figure 25 Maximum displacement magnitude (m) around the wellbore for the interval of 3861-3865 m with mud pressure equal to 67.4 MPa.

Table 10 Displacements (m) in horizontal stresses direction by applying different mud weights for the range 3861-3865 m.

Mud pressure (MPa)	64	66	67	67.4	68.18	71
Displacement in maximum horizontal stress direction (m)	8.32 e-3	6.98 e-4	3.33 e-4	2.18 e-4	1.62 e-4	7.28 e-5
Displacement in minimum horizontal stress direction (m)	8.48 e-3	7.92 e-4	3.55 e-4	2.81 e-4	2.31e-04	1.47 e-4

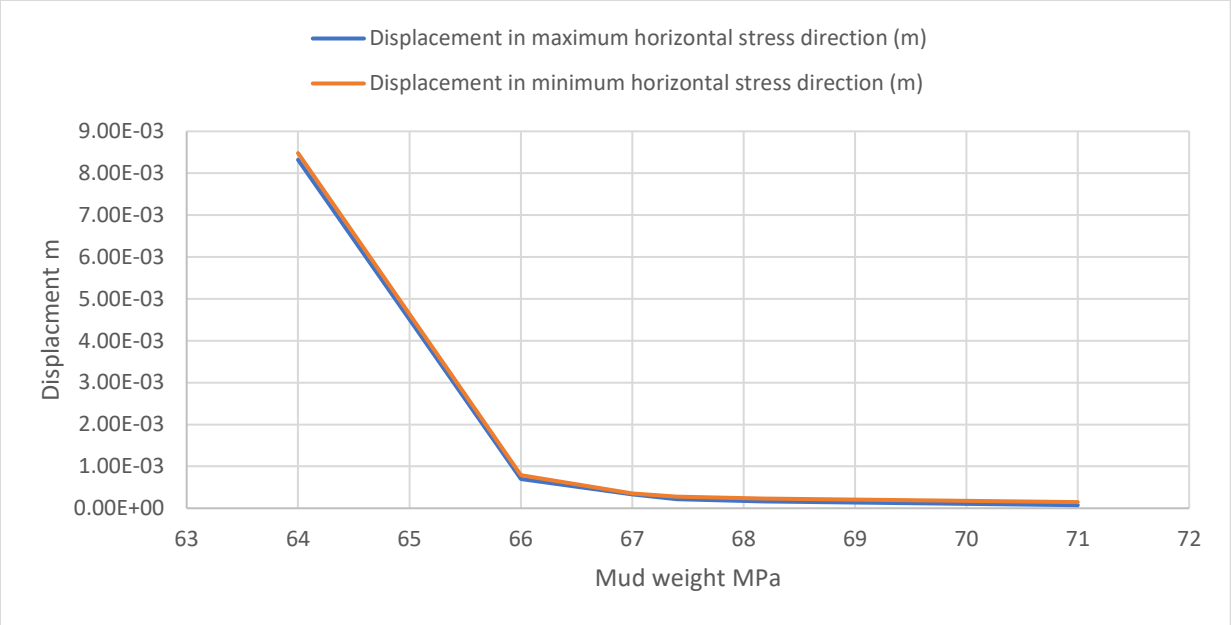

Figure 26 reducing displacement in both maximum and minimum horizontal stress direction (m) by increase in mud weight for interval of 3861-3865 m.

3.4. NYZA results in reservoir section

Five intervals were selected for calculation of the NYZA values correspondent to each mud weight applied to the model, at the reservoir section of the nominated well. The values listed in Table 11 were used as rock properties and stress magnitudes of the surrounding rock. These values are the outputs of 1D MEM, which was built in the previous section for the well at the depth of modeling.

Table 11 Input parameters for modeling of five depth intervals of the reservoir section.

Depth	υ	μ	Ø	K	C	E	Tensile strength	Pp	Mud Pressure	ρ	Sv	SHmax	Shmin
M		GPa	degree	GPa	MPa	GPa	MPa	MPa	MPa	Kg/m3	MPa	MPa	MPa
3807-3811	0.3	8.7	45	14.5	11	21.7	11.23	68	68.71	2980	93	95.56	81.35
3842-3846	0.3	3.4	43	9.17	8.6	9.3	6.3	68.1	70.6	2870	94.5	93.07	82.7
3861-3865	0.3	3.9	31.5	7.9	4.1	10	3.7	68.2	71.92	2400	94.9	84.8	79.9
3928-3932	0.2	5.9	46	9.1	9.2	14.7	6.8	68.3	72.27	2738	96.5	95.83	81.35
4036-4040	0.2	4.8	40.2	10.3	5.35	12.1	5.59	63.1	72.3	2789	99.6	89.08	80.45

The calculations conducted at different mud pressures for each selected interval are shown in the following (Figure 27, Figure 28, Figure 29, Figure 30, Figure 31). An exponential curve was fitted to the results to interpolate the mud pressure corresponding to NYZA=1.

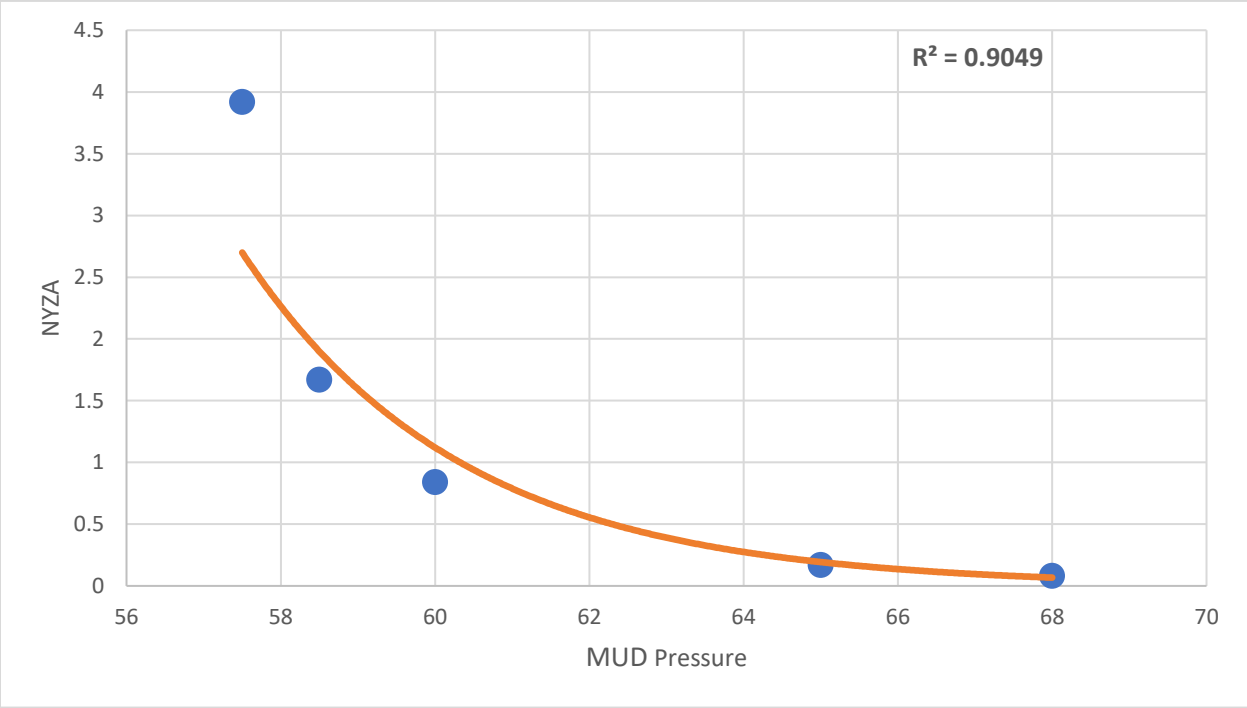

Figure 27 NYZA vs. mud pressure MPa for depth interval 3708-3711 m.

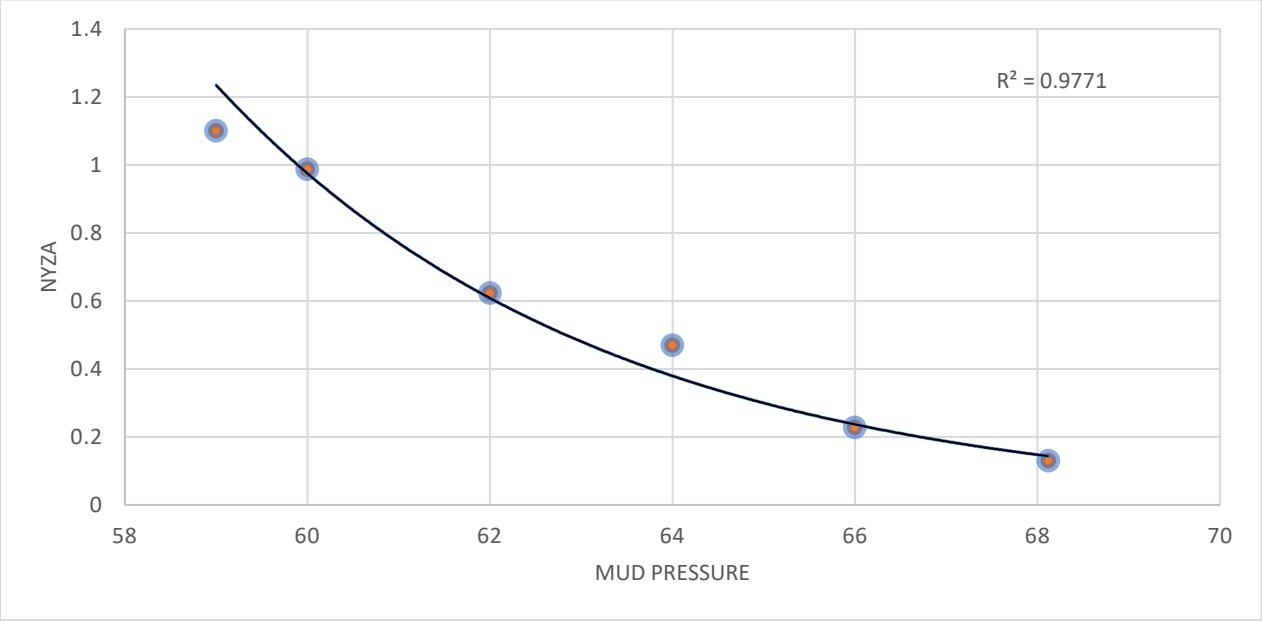

Figure 28 NYZA vs. mud pressure MPa for depth interval 3842-3846 m.

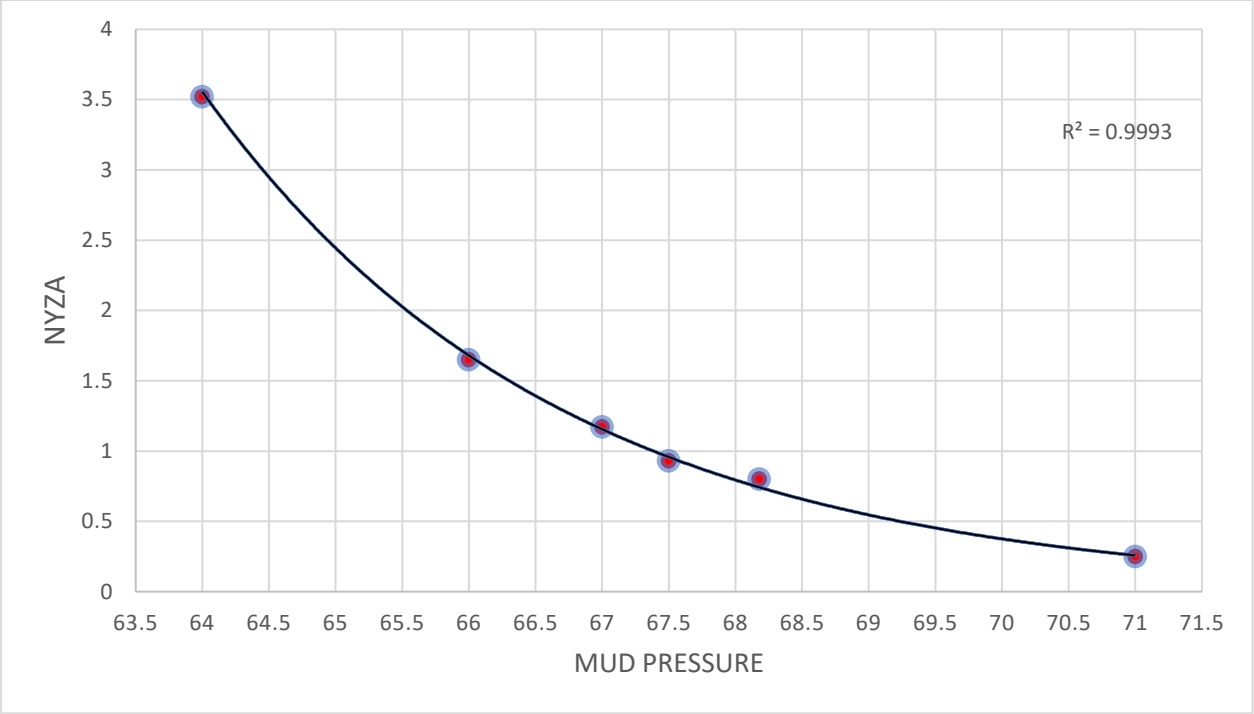

Figure 29 NYZA vs. mud pressure MPa for depth interval 3861-3865 m.

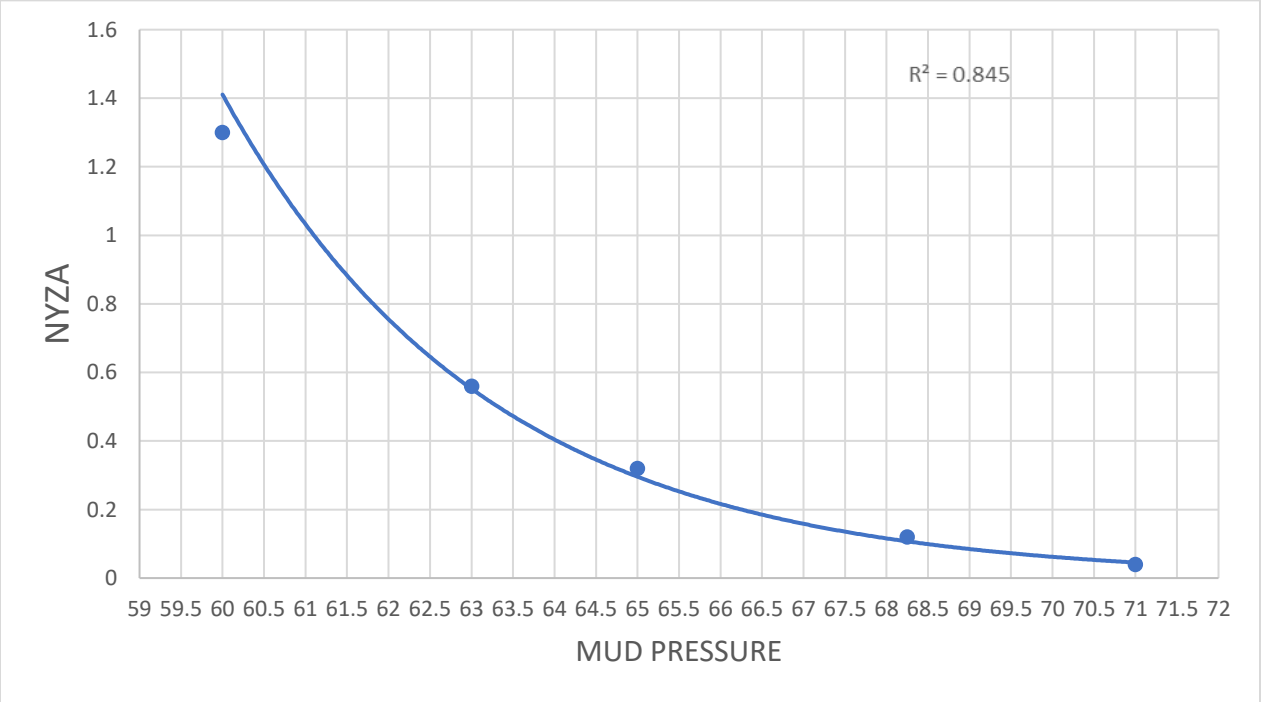

Figure 30 NYZA vs. mud pressure MPa for depth interval 3928-3932 m.

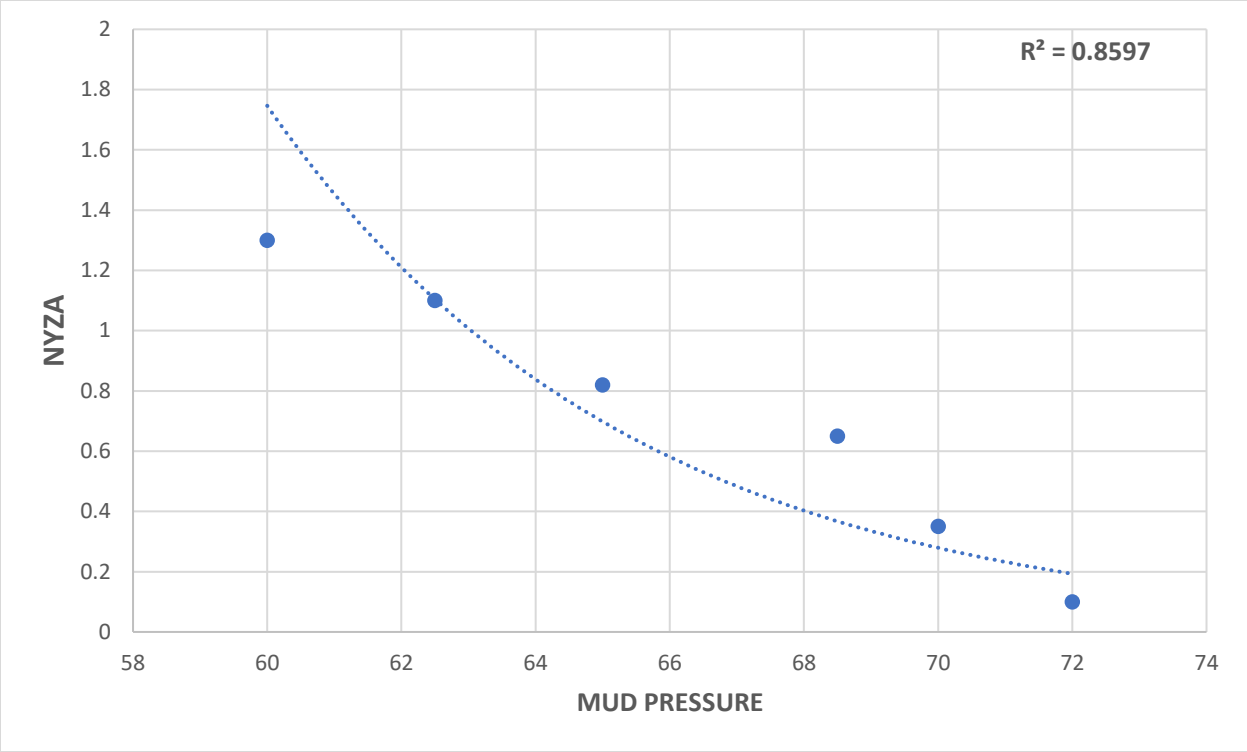

Figure 31 NYZA vs. mud pressure MPa for depth interval 4036-4040 m.

After running the model for each interval, the corresponding NYZA values were obtained and recorded in Table 12. By considering the optimum mud weights corresponding to NYZA=1 and comparing it with pore pressures, it can be inferred that the reservoir section could be drilled under an UBD condition. The estimated optimum mud weights by FLAC 3D for the studied five intervals are illustrated in Figure 32 as black solid circles.

Table 12 Mud pressures and weights corresponding to NYZA=1 for all reservoir intervals.

Depth (M)	**4036-4040**	**3928-3932**	**3861-3865**	**3842-3846**	**3807-3811**
Mud pressure corresponding to NYZA=1 (MPa)	63.4	61	67.4	59.7	60.2
Mud pressure used while drilling (MPa)	72.3	72.27	71.92	70.6	68.71
Mud weight used while drilling (ppg)	15.23	15.64	15.83	15.62	15.34
Mud weight corresponding to NYZA=1 (ppg)	13.35	13.2	14.84	13.21	13.44
Pore pressure (MPa)	68.29	68.25	68.18	68.12	68

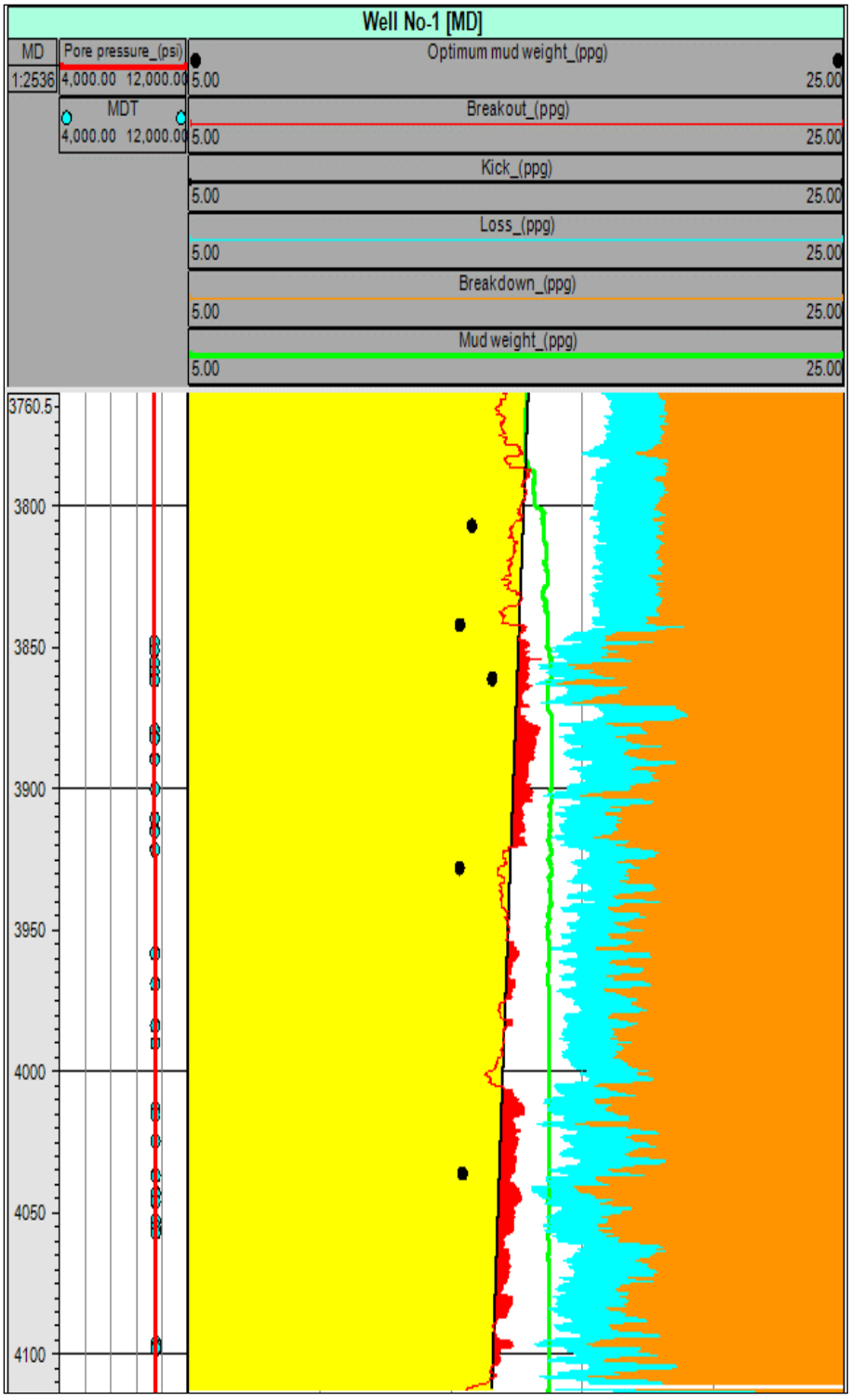

Figure 32 From Left: reservoir pore pressure profile and MDT results; safe mud window derived from 1D MEM Model through the wellbore, as well as the applied drilling mud weight for well.

3.5. NYZA Results in non-reservoir section

A safe mud weight window is conventionally determined and used to support drillers in avoiding possible operational losses. In this study, there are non-reservoir zones where a safe mud weight window could not be established. The rock elastic and mechanical properties for the non-reservoir sections are derived from the mechanical earth model (1D MEM) which was calibrated thanks to the core results and was built specifically for the well. The properties that have been extracted from 1D MEM model are listed in Table 13.

Table 13 Input parameters for modeling of two non-reservoir intervals with no safe mud weight window.

Depth	υ	μ	Ø	K	C	E	Tensile strength	Pp	Mud Pressure	ρ	Sv	σh	Shmin
M		GPa	degree	GPa	MPa	GPa	MPa	MPa	MPa	Kg/m3	MPa	MPa	MPa
2576-2580	0.3	2.1	30	5.47	3.66	5.58	2.38	31.3	27.4	2643	61.1	50.97	46.93
3550-3554	0.3	1.2	29.53	4.13	1.9	2.89	2.73	59.8	63.85	2378	87.2	70.56	72.62

The applied approach was also used for 2618-2622 m and 3580-3584 m intervals in which there is no safe mud weight window exist on 1D MEM model. For these ranges, optimal mud weights were determined and plotted to represent optimal weight or the mud weight with minimal instability problems during drilling operations (see Figure 33 and Figure 34).

Since there was no MDT or XPT tools runs in this section (common practice in oil and gas industry is to run the pressure measurement tools only in reservoir section i.e., XPT or MDT unless it is required which was not this well case) the pore pressure was calculated as described in section 2.7. Lack of shale in some intervals may lead to some uncertainty for computed pore pressure profile. Therefore, the pore pressure profile and consequently stresses may be affected by this ambiguity. The way to reduce this effect is to apply the drilling event and the weight of the mud that was used for the well and the calibration tools. The points that have been select have such characteristic.

Figure 35 shows the mud weight windows and its components for these two sections as well as drilling mud weight for well a (2618-2622) and b (3580-3584). For these ranges, the mud weights had been determined and plotted to represent the optimum mud weight or the mud weight with minimal instability problems during drilling operations.

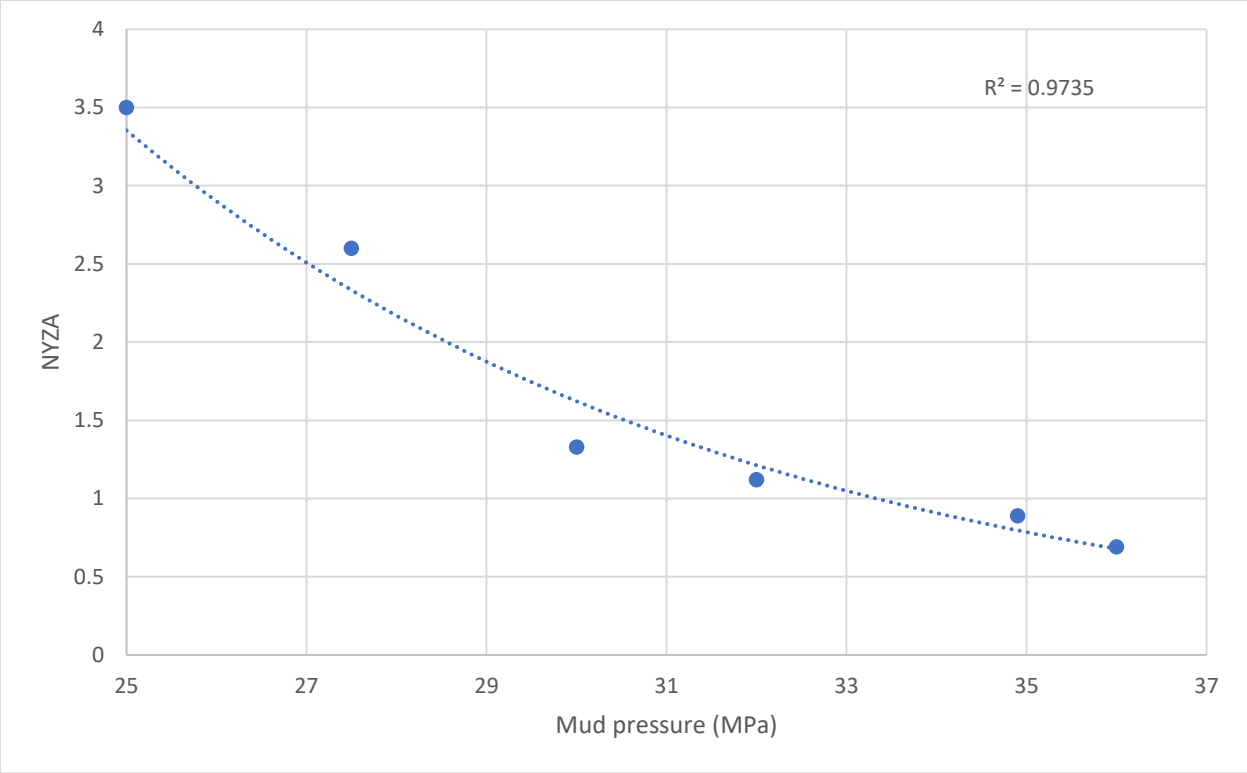

Figure 33 NYZA vs. mud pressure MPa for depth interval 2618-2622m

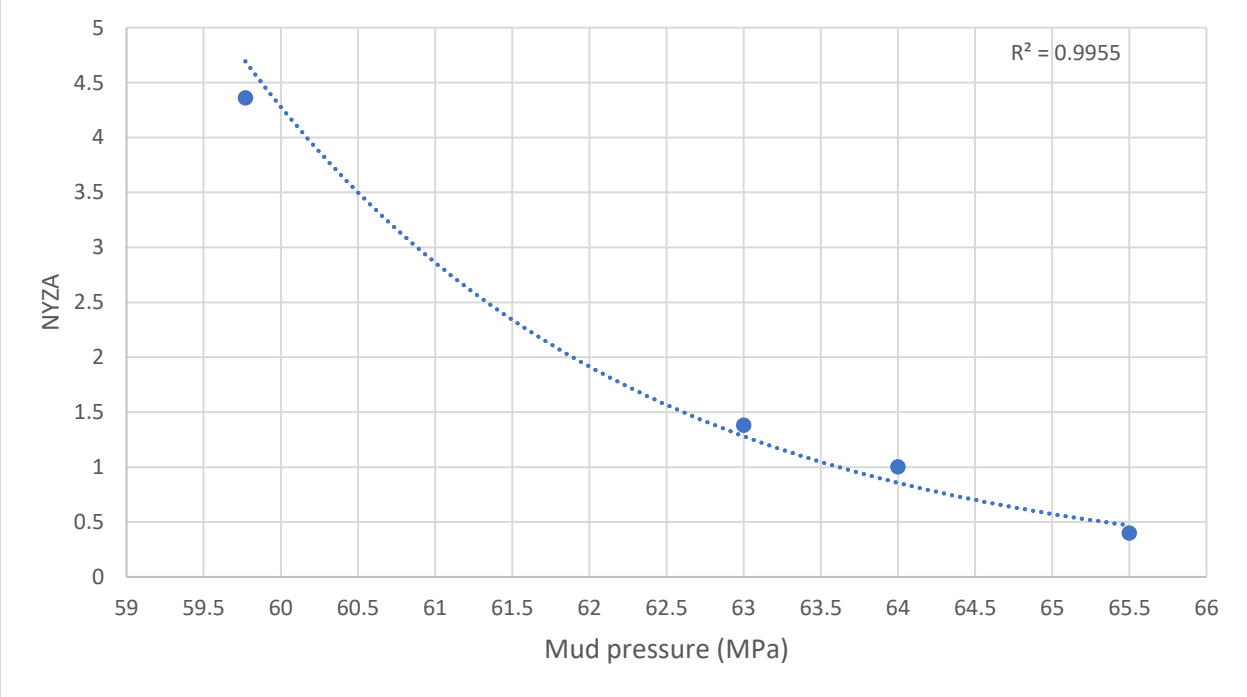

Figure 34 NYZA vs. mud pressure MPa for depth interval 3580-3584m.

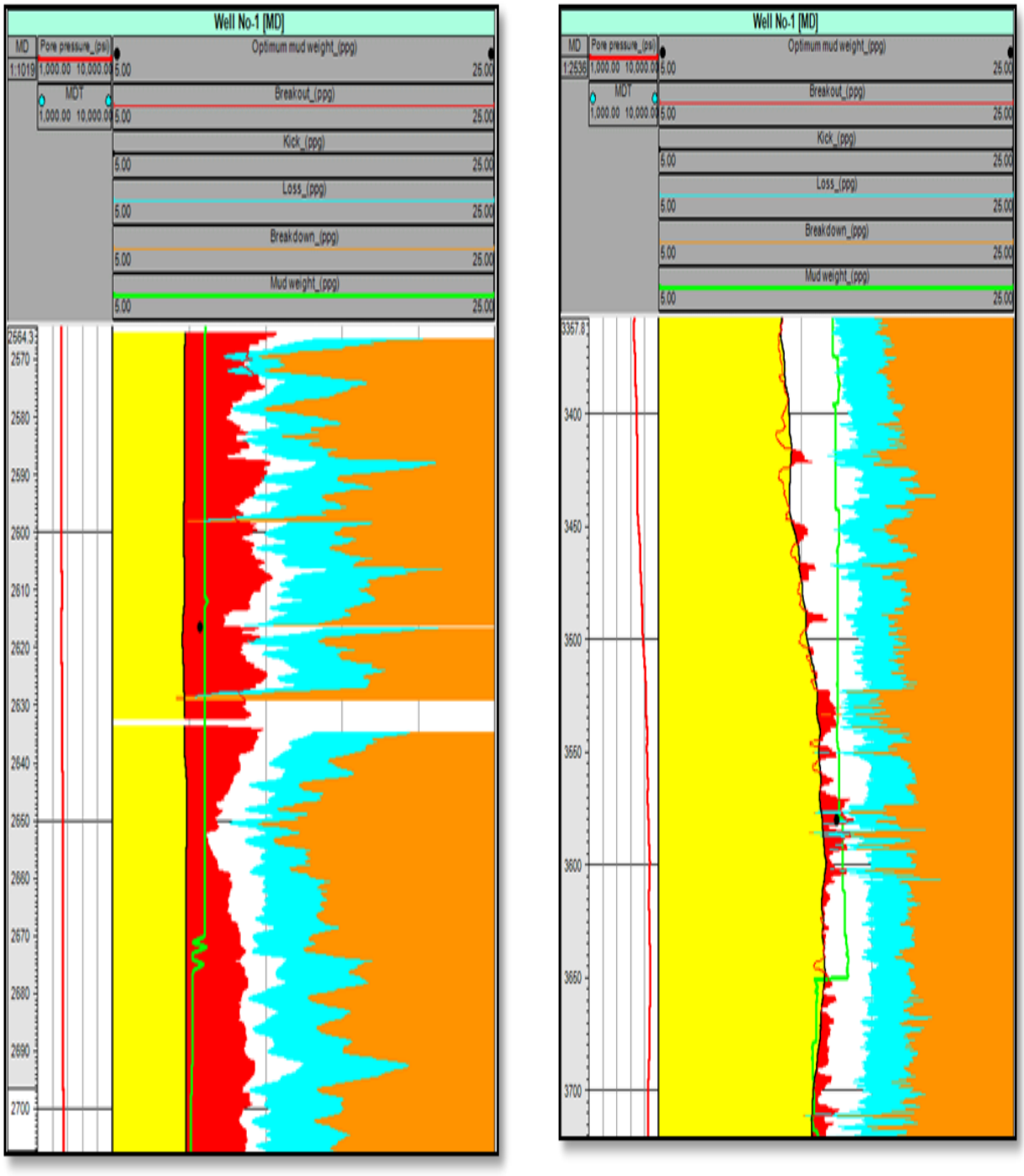

a)

b)

Figure 35 From Left: pore pressure profile through the wellbore and MDT results; safe mud window derived from 1D MEM Model through the wellbore, as well as the applied drilling mud weight for well; a) (2618-2622); b) (3580-3584).

After running the model for each interval, the corresponding NYZA values were obtained and recorded in Table 14 By considering the optimum mud weights corresponding to NYZA=1 and comparing it with pore pressures, it can be inferred that the non-reservoir section can be drilled under managed pressure drilling to increase the wellbore stability. The estimated optimum mud weights by FLAC 3D for the non-reservoir section studied can be assumed to be optimum mud weight for these two intervals.

Table 14 Mud weights correspond to NYZA=1 for two non-reservoir intervals with no safe mud weight window.

Depth (M)	**2618-2622**	**3580-3584**
Mud pressure corresponding to NYZA=1 (MPa)	33.1	63.7
Mud pressure used while drilling (MPa)	32	63.85
Mud weight used while drilling (ppg)	10.46	15.12
Mud weight corresponding to NYZA=1 (ppg)	10.8	15.16
Pore pressure (MPa)	31.26	59.77

4. Conclusion and discussion

4.1. Limitations

in this study, there are a number of specific restrictions associated with the process, that are summarized as follows:

1. Some intervals are poorly logged due to inherent of sonic logs that should be acquired in the open hole, and the likelihood of these intervals being affected by fracture or some discontinuities like faults or the skin damages that might occur during the drilling or any other artifacts. These will result in some spike or some null value in the primitive log data. The work has been done to compensate these artifacts by normalizing the log data removing some sharp trends and de spiking the sonic and density log out puts.
2. The 1D Geomechanical model has been built through log derived parameters with limited core calibration (reservoir section only).
3. For calculation of rock properties, the correlation obtained from the core data has been used. Since this correlation was related to the reservoir section, this may add some uncertainties to the MEM constructed for the non-reservoir section.
4. For the over-burden calculation, some extrapolation was required, since the density log was not available from the top.
5. Conservative Mohr-Coulomb failure criteria were used for all Mud Weight window calculations.
6. The values used for ε_x and ε_y were respectively 0.1 and 0.9. These values were choosen based on the literature review and history matching with the events in the well.
7. The generally high level of losses found in the drilled well cannot be easily explained by the standard wellbore stability models, where the calculated mud weight windows are positive. These losses may be caused by the presence of open features such as faults, fractures, or karsts bridged by minerals. These losses were not used for calibration and history matching of the models.
8. Chemical based failure has not been considered. This can occur when an incompatible fluid in the wellbore causes adverse reactions with the rock matrix or formation fluids leading to material expansion or unwanted reaction products.

9. When it comes to decide for the well drilling method, several factors such as the economic factor, the environmental factor, the safety issue, the logistic and etc. will play an important role. This study did not focus on any of these highly important factors to make a decision for such operation, but its aim was to deliver the method that can be used for the feasibility study of the underbalanced drilling.

4.2. MEM results

During drilling, borehole breakouts and drilling induced fractures (breakdowns) are the two main instability problems which may lead to stuck pipe, reaming operations, sidetracking, and loss of circulation. These problems can be often addressed by selecting a suitable mud weight for drilling. To evaluate the stability of a wellbore, an accurate model is required, to compute the stresses around the borehole. Chapter 2 was dedicated to build the mechanical earth model for the purpose of wellbore stability analysis. The work was performed using all available data acquired for the well. The constructed 1D MEM then calibrated with the drilling events and measurements available. Following are the results that can be interpreted from 1D MEM of the well.

1. In the current study, conversion of dynamic to static Young's moduli (YME) took place using extracted correlation from test results. The alternative was to use the existed equation in the literature. The method shows a good match, and the results are reasonable for the non-reservoir section.
2. For Poisson's ratio, log-derived values calibrated using triaxial compression test's results then converted to static value show fair match.
3. For UCS and tensile strength of the rock the core results correlation distribution throughout the model shows promising outputs.
4. The poroelastic horizontal strain model with values for ε_x and ε_y respectively 0.1 and 0.9 was matched with the events in well.
5. The initial stress computation using procedure describe in section 2 reveals that the stress regime is normal ($\sigma_v > \sigma_H > \sigma_h$) toward strike-slip ($\sigma_H > \sigma_v > \sigma_h$).
6. Mud weight windows that have been derived from MEM, reveals that for the most part of the well, exist a wide spectrum of safe margin for drilling without encountering any drilling problems i.e., loss, breakout, or hydraulically fracture zone.

7. In some intervals the safe mud windows will be shrunk and reach the negative value. A negative mud weight window is the phenomenon that should be managed by the drilling engineer. The MEM will help the planning of such problematic sections prior.
8. MEM that has been constructed in the section 2 can be used for the optimization the deviated and horizontal well design if needed so.
9. The MEM can be used for further sand production or subsidence study as well.

4.3. UBD feasibility results

Different wellbore stability models are often numerically solved by finite explicit or finite element methods. Herein, a finite explicit simulator, FLAC 3D, was employed to conduct the wellbore stability simulation. An elastoplastic model coupled with Mohr-Coulomb failure criterion was used in FLAC 3D to assess stability conditions with respect to different mud weights. The growth of yielded/plastic zone around the wellbore was used to analyze the risk of wellbore instability. In section 3, the normalized yielded zone area (NYZA) was used as an indicator for growth of the plastic zone which is the ratio of the cross-sectional area of the plastic zone to original area of the wellbore. Different NYZA values with respect to different mud weights were plotted and the best curve was fitted to the results. Mud weight corresponds to NYZA=1 was the optimum mud weight.

1. As per this case study, the feasibility of underbalanced drilling in high pore pressure reservoirs can be investigated using the suggested NYZA index.
2. In high-pressure reservoirs like this, safety issues may arise due to large influx of formation fluids. This problem occurs when unexpected high pressure or high permeability areas are reached. Using this method will identify these areas prior to drilling, and it will be possible to plan the handling of fluids at the surface.
3. For the reservoir section, the method reveals the possibility of underbalanced drilling for a gas reservoir with over 9000 psi reservoir pressure that has already drilled over balanced.
4. Being able to drill underbalanced may lead to enhanced recovery, reducing formation damage and increasing intra-zone contribution, increase drainage area and rate of penetration or avoiding differential sticking as benefits of the method that can be considered for the next well drilling option.

5. The method developed in this work determined the optimum mud weights in two intervals where there were no possible safe mud weight windows. For such problematic ranges, the method provides the mud weights in which the well will have the minimum instability problems during drilling.
6. The suggestions of the method developed are consistent with the best applied drilling operations in the field. As a result, the method is also good in introducing the optimum mud weights for cases where there are narrow or no safe mud weight windows.

4.4. Recommendation

1. Further work is recommended to study the quantitative relationship between the onset of instability problems and the critical value of NYZA by taking account for the live data in the field.
2. While the plane strain assumption is commonly used for the wellbore stability analysis, it is not naturally applicable for all wellbore conditions. 3D modeling is necessary for more complicated wellbore profiles.
3. Good performance of a numerical simulation relies on the good quality of data, including the in-situ stress and a series of rock mechanical data. However, data collection is usually difficult for a real field. Further effort is recommended to retrieve field data more accurately and at lower cost.
4. Mohr–Coulomb Failure Criterion has been used in this study as a conservative criterion. The procedure can be repeated using different criteria to compare the results.
5. Most reliable data in such modeling comes from geomechanical analysis of core data. Core drilling inherently considers a potential risk when drilling. This will result in the oil and gas company's reluctance to recover the core. Hence, most companies are inclined to recover the cores only when necessary and mainly in the section of the reservoir. For a good quality MEM that can lead to better understanding of the subsurface and plan less expensive drilling operation in the future, this attitude should change.

Reference

1. Aadnoy, B. and M. Chenevert (1987). "Stability of highly inclined boreholes (includes associated papers 18596 and 18736)." SPE Drilling Engineering **2**(04): 364-374.
2. Aadnoy, B. S., I. Cooper, S. Miska, R. F. Mitchell and M. L. Payne (2009). Advanced drilling and well technology, SPE Richardson, Texas.
3. Aadnoy, B. S. and U. S. o. P. Engineers (2009). Advanced drilling and well technology, SPE.
4. Aghajanpour, A., S. H. Fallahzadeh, S. Khatibi, M. M. Hossain and A. Kadkhodaie (2017). "Full waveform acoustic data as an aid in reducing uncertainty of mud window design in the absence of leak-off test." Journal of Natural Gas Science and Engineering **45**: 786-796.
5. Ajah, N., A. Dosunmu, C. Akaolisa and T. Dagogo (2020). "Analysis of Elastic Geomechanical Properties Derived From Well Log and Seismic Data, Using Artificial Intelligence (ANN): A Case Study of "AJAH" Field Offshore Niger Delta." IOSR Journal of Applied Geology and Geophysic **8**: 19-27.
6. Al-Ajmi, A. M. and R. W. Zimmerman (2005). "Relation between the Mogi and the Coulomb failure criteria." International Journal of Rock Mechanics and Mining Sciences **42**(3): 431-439.
7. Al-Ajmi, A. M. and R. W. Zimmerman (2009). "A new well path optimization model for increased mechanical borehole stability." Journal of Petroleum Science and Engineering **69**(1-2): 53-62.
8. Al-Shaaibi, S. K., A. M. Al-Ajmi and Y. Al-Wahaibi (2013). "Three dimensional modeling for predicting sand production." Journal of Petroleum Science and Engineering **109**: 348-363.
9. Alexeyev, A., M. Ostadhassan, R. A. Mohammed, B. Bubach, S. Khatibi, C. Li and L. Kong (2017). Well log based geomechanical and petrophysical analysis of the bakken formation. 51st US Rock Mechanics/Geomechanics Symposium, American Rock Mechanics Association.
10. Ali, A. H. A. (2003). "Watching rocks change-mechanical earth modeling." Oilfield Review, summer **15**: 22-39.
11. Alquwizani, S. and M. Sharma (2014). Three-Dimensional Modeling of Wellbore and Perforation Stability in Weak Sands. SPE International Symposium and Exhibition on Formation Damage Control, Society of Petroleum Engineers.
12. Alquwizani, S. A. (2013). "Three-dimensional elasto-plastic modeling of wellbore and perforation stability in poorly consolidated sands."

13. Anderson, E. M. (1905). "The dynamics of faulting." Transactions of the Edinburgh Geological Society **8**(3): 387-402.
14. Bérard, T. and R. Prioul (2016). "Mechanical Earth Model." Oilfield Review. The Defining Series.
15. Blanton, T. and J. E. Olson (1999). "Stress magnitudes from logs: effects of tectonic strains and temperature." SPE Reservoir Evaluation & Engineering **2**(01): 62-68.
16. Bowers, G. L. (1995). "Pore pressure estimation from velocity data: Accounting for overpressure mechanisms besides undercompaction." SPE Drilling & Completion **10**(02): 89-95.
17. Bradford, I. D. R. and J. Cook (1994). A semi-analytic elastoplastic model for wellbore stability with applications to sanding. Rock Mechanics in Petroleum Engineering, Society of Petroleum Engineers.
18. Bradford, I. D. R. and J. M. Cook (1994). A semi-analytic elastoplastic model for wellbore stability with applications to sanding. Rock Mechanics in Petroleum Engineering. Delft, Netherlands, Society of Petroleum Engineers**:** 8.
19. Bradley, W. (1979). "Mathematical concept-Stress Cloud-can predict borehole failure." Oil Gas J.;(United States) **77**(8).
20. Capasso, G. and G. Musso (2010). Evaluation of Stress and Strain Induced by the Rock Compaction on a Hydrocarbon Well Completion Using Contact Interfaces with Abaqus. Proc. ABAQUS Users' Conference, Providence RI, USA.
21. Castagna, J. P. and S. Sun (2006). "Comparison of spectral decomposition methods." First break **24**(3).
22. Chardac, O., D. Murray, A. J. G. Carnegie and R. Marsden (2005). A proposed data acquisition program for successful geomechanics projects. SPE Middle East Oil and Gas Show and Conference, OnePetro.
23. Chen, S. and Y. Abousleiman (2016). "Drained and undrained analyses of cylindrical cavity contractions by bounding surface plasticity." Canadian Geotechnical Journal **53**(9): 1398-1411.
24. Choi, S. and C. Tan (1998). Modelling of effects of drilling fluid temperature on wellbore stability. SPE/ISRM Rock Mechanics in Petroleum Engineering, OnePetro.

25. Crook, A. J. L., J.-G. Yu and S. M. Willson (2002). Development of an Orthotropic 3D Elastoplastic Material Model for Shale. SPE/ISRM Rock Mechanics Conference. Irving, Texas, Society of Petroleum Engineers**:** 10.
26. Cui, L. (1997). "Poroelastic Solution for an." Journal of applied mechanics **64**: 33.
27. Cui, L., Y. Abousleiman, A. H. Cheng and J.-C. Roegiers (1999). "Time-dependent failure analysis of inclined boreholes in fluid-saturated formations."
28. Deangeli, C. and M. Marchelli "Combined Effect of Pore Water Overpressure, Far-Field Stresses, and Strength Parameters in Wellbore Stability." Frontiers in Earth Science: 353.
29. Detournay, E. and A. Cheng (1987). "Linear poroelasticity and rock mechanics applications." Int. J. Rock Mech. & Mining Sciences.
30. Eaton, B. A. (1975). The equation for geopressure prediction from well logs. Fall meeting of the Society of Petroleum Engineers of AIME, OnePetro.
31. Eck-Olsen, J., E. Vollen and T. Tønnessen (2004). Challenges in implementing ubo technology. SPE/IADC Underbalanced Technology Conference and Exhibition, Society of Petroleum Engineers.
32. Ewy, R., P. Ray, C. Bovberg, P. Norman and H. Goodman (1999). Openhole stability and sanding predictions by 3D extrapolation from hole collapse tests. SPE Annual Technical Conference and Exhibition, Society of Petroleum Engineers.
33. Foster, J. (1966). "Whalen." HE Estimation of formation pressures from electrica1 surveys-Offshore Louisiana **18**(2): 165-161.
34. Fuh, G.-F., D. Whitfill and P. Schuh (1988). Use of borehole stability analysis for successful drilling of high-angle hole. IADC/SPE Drilling Conference, OnePetro.
35. Hareland, G. and K. K. Dehkordi (2007). Wellbore Stability analysis in UBD Wells of Iranian fields. SPE Middle East Oil and Gas Show and Conference, Society of Petroleum Engineers.
36. Hawkes, C. D. and P. J. McLellan (1996). Modeling of Yielded Zone Enlargement Around a Wellbore. 2nd North American Rock Mechanics Symposium. Montreal, Quebec, Canada, American Rock Mechanics Association**:** 8.
37. Hawkes, C. D. and P. J. McLellan (1999). "A new model for predicting time-dependent failure of shales: theory and application." Journal of Canadian Petroleum Technology **38**(12).

38. Hawkes, C. D., S. Smith and P. McLellan (2002). Coupled Modeling of Borehole Instability and Multiphase Flowfor Underbalanced Drilling. IADC/SPE Drilling Conference, Society of Petroleum Engineers.
39. He, S., W. Wang, H. Shen, M. Tang, H. Liang and J. a. Lu (2015). "Factors influencing wellbore stability during underbalanced drilling of horizontal wells–When fluid seepage is considered." Journal of Natural Gas Science and Engineering **23**: 80-89.
40. Hsiao, C. (1988). Growth Of Plastic Zone In Porous Medium Around A Wellbore. Offshore Technology Conference. Houston, Texas, Offshore Technology Conference**:** 10.
41. Inc., T. (1998). "The Difference Between Static and Dynamic Mechanical Properties." TerraTek Standard Publications.
42. Khatibi, S., A. Aghajanpour, M. Ostadhassan and O. Farzay (2018). "Evaluating Single-Parameter parabolic failure criterion in wellbore stability analysis." Journal of Natural Gas Science and Engineering **50**: 166-180.
43. Khatibi, S., O. Farzay and A. Aghajanpour (2018). A Method to Find Optimum Mud Weight in Zones With No Safe Mud Weight Windows. 52nd US Rock Mechanics/Geomechanics Symposium, American Rock Mechanics Association.
44. Khatibi, S., M. Ostadhassan, O. Farzay and A. Aghajanpour (2019). Seismic Driven Geomechanical Studies: A Case Study in an Offshore Gas Field. 53rd U.S. Rock Mechanics/Geomechanics Symposium. New York City, New York, American Rock Mechanics Association**:** 6.
45. Kim, A. S. and M. M. Sharma (2012). A Predictive Model For Sand Production In Realistic Downhole Condition. 46th U.S. Rock Mechanics/Geomechanics Symposium. Chicago, Illinois, American Rock Mechanics Association**:** 7.
46. Malloy, K. P., R. Stone, G. H. Medley, D. M. Hannegan, O. D. Coker, D. Reitsma, H. M. Santos, J. I. Kinder, J. Eck-Olsen and J. W. McCaskill (2009). Managed-pressure drilling: What it is and what it is not. IADC/SPE Managed Pressure Drilling and Underbalanced Operations Conference & Exhibition, OnePetro.
47. McLean, M. and M. Addis (1990). Wellbore stability analysis: a review of current methods of analysis and their field application. IADC/SPE drilling conference, OnePetro.
48. McLean, M. and M. Addis (1990). Wellbore stability: the effect of strength criteria on mud weight recommendations. SPE annual technical conference and exhibition, OnePetro.

49. McLellan, P. (1996). "Assessing the risk of wellbore instability in horizontal and inclined wells." Journal of Canadian Petroleum Technology **35**(05).
50. McLellan, P., C. Hawkes and R. Read (2000). Sand production prediction for horizontal wells in gas storage reservoirs. SPE/CIM International Conference on Horizontal Well Technology, Society of Petroleum Engineers.
51. McLellan, P. and Y. Wang (1994). Predicting the effects of pore pressure penetration on the extent of wellbore instability: application of a versatile poro-elastoplastic model. Rock mechanics in petroleum engineering, OnePetro.
52. McLellan, P. J. and C. D. Hawkes (1999). Borehole Stability Analysis For Underbalanced Drilling. Annual Technical Meeting. Calgary, Alberta, Petroleum Society of Canada**:** 15.
53. Mody, F. K. and A. H. Hale (1993). "Borehole-stability model to couple the mechanics and chemistry of drilling-fluid/shale interactions." Journal of Petroleum Technology **45**(11): 1093-1101.
54. Molaghab, A., M. H. Taherynia, S. M. Fatemi Aghda and A. Fahimifar (2017). "Determination of minimum and maximum stress profiles using wellbore failure evidences: a case study—a deep oil well in the southwest of Iran." Journal of Petroleum Exploration and Production Technology **7**(3): 707-715.
55. Papanastasiou, P. and A. Zervos (2005). Applications of computational geomechanics in petroleum engineering.
56. Pašić, B., N. Gaurina-Međimurec and M. Davorin (2007). "Wellbore instability: Causes and consequences." Rudarsko-Geološko-Naftni Zbornik **19**.
57. Pašić, B., N. Gaurina Međimurec and D. Matanović (2007). "Wellbore instability: causes and consequences." Rudarsko-geološko-naftni zbornik **19**(1): 87-98.
58. Plona, T. and J. Cook (1995). Effects of stress cycles on static and dynamic Young's moduli in Castlegate sandstone. The 35th US Symposium on Rock Mechanics (USRMS), OnePetro.
59. Plumb, D., H. Krabbe, J. Rasmus, Q. Li, T. Bornemann and T. Bratton (1999). Logging-While-Drilling Images For Geomiechanical, Geological And Petrophysical Interpretations. SPWLA 40th Annual Logging Symposium, OnePetro.
60. Rahman, K., A. Khaksar and T. J. Kayes (2010). "An integrated geomechanical and passive sand-control approach to minimizing sanding risk from openhole and cased-and-perforated wells." SPE Drilling & Completion **25**(02): 155-167.

61. Risnes, R., R. K. Bratli and p. Horsrud (1981). Stress around a Wellbore. SPE 9650. Manama, Bahrain SPE Middle East Oil Technical Conference.
62. Salehi, S., G. Hareland and R. Nygaard (2010). "Numerical simulations of wellbore stability in under-balanced-drilling wells." Journal of Petroleum Science and Engineering **72**(3-4): 229-235.
63. Santarelli, F., E. Brown and V. Maury (1986). Analysis of borehole stresses using pressure-dependent, linear elasticity. International Journal of Rock Mechanics and Mining Sciences & Geomechanics Abstracts, Elsevier.
64. Saponja, J. (1998). "Challenges with jointed pipe underbalanced operations." SPE drilling & completion **13**(02): 121-128.
65. Sherwood, J. (1993). "Biot poroelasticity of a chemically active shale." Proceedings of the Royal Society of London. Series A: Mathematical and Physical Sciences **440**(1909): 365-377.
66. Soliman, M. and P. Boonen (2000). "Rock mechanics and stimulation aspects of horizontal wells." Journal of Petroleum Science and Engineering **25**(3-4): 187-204.
67. Urselmann, R., J. Cummins, R. Worrall and G. House (1999). Pressured mud cap drilling: efficient drilling of high-pressure fractured reservoirs. SPE/IADC Drilling Conference, Society of Petroleum Engineers.
68. Wang, Y. (1998). Onset of sand production and open hole stability near heated horizontal wells. SPE/ISRM Rock Mechanics in Petroleum Engineering, OnePetro.
69. Wang, Y. and M. B. Dusseault (1995). "Response of a circular opening in a friable low-permeability medium to temperature and pore pressure changes." International Journal for numerical and analytical methods in geomechanics **19**(3): 157-179.
70. Wang, Y. and E. Papamichos (1994). "Conductive heat flow and thermally induced fluid flow around a well bore in a poroelastic medium." Water Resources Research **30**(12): 3375-3384.
71. Wang, Y., E. Papamichos and M. B. Dusseault (1996). Thermal stresses and borehole stability. 2nd North American Rock Mechanics Symposium, OnePetro.
72. Westergaard, H. M. (1940). "Plastic state of stress around a deep well."
73. Yew, C. and G. Liu (1992). Pore fluid and wellbore stabilities. International Meeting on Petroleum Engineering, OnePetro.
74. Yew, C. H., M. E. Chenevert, C. L. Wang and S. Osisanya (1990). "Wellbore stress distribution produced by moisture adsorption." SPE Drilling engineering **5**(04): 311-316.

75. Zeynali, M. E. (2012). "Mechanical and physico-chemical aspects of wellbore stability during drilling operations." Journal of Petroleum Science and Engineering **82**: 120-124.
76. Zhou, S., R. Hillis and M. Sandiford (1996). "On the Mechanical Stability of lnclined Wellbores." SPE Drilling & Completion **11**(02): 67-73.